



Steel plate shear walls with partial length connection to vertical boundary element

Mohammad Reza Haji Mirsadeghi, Nader Fanaie*

Department of Civil Engineering K. N. Toosi University of Technology, Tehran Iran

ARTICLE INFO

Keywords:

Steel plate shear wall
 Partial length infill plate connection
 Experimental and numerical investigation
 Vertical boundary element
 Tension field inclination angle
 Developing governing equations

ABSTRACT

This research project aims to propose an innovative analytical method to evaluate steel plate shear wall with partial length connection to vertical boundary element which lacks the connection at the middle height of VBE. In this type of steel shear walls, reducing the length of the connection between infill and vertical boundary element results in a reduction in the flexure and stiffness demand on the vertical boundary elements. Push-over loading was carried out on four small-scale designed test specimens so as to investigate the quality of tension field formation in web plate by changing not connected length ratio. Then numerical model was employed to develop comprehensive study on web plate stress state due to the formation of tension field by changing not connected length ratio. Firstly, the formation of parallel tension strips in the infill plate of the steel shear wall with different partial length connections to vertical boundary elements in specified range of lack of connection was confirmed. Based on aforementioned experimental and numerical study evidence, governing equations have been developed for this analytical solution, including panel shear strength, tension field inclination angle and minimum stiffness requirements in vertical boundary elements.

1. Introduction

Steel plate shear wall (SPSW) is a lateral load resisting system capable of effectively bracing a building against both wind and earthquake excitations. It was introduced about fifty years ago [1]. Despite all evidence presented by researchers [2–7] regarding its suitable and ductile behavior against lateral loads it is not being extensively utilized. It is believed by many researchers [8] that the most important reason for the lack of widespread application of this system is attributed to the unconventional dimension of the vertical boundary elements (VBE). Due to the formation of the tension field and framing action of the boundary element, as well as satisfying the minimum flexural stiffness required for vertical boundary elements to form an almost uniform tension field, large flexural and axial demands have led to the selection of large and unconventional dimensions for these elements [8]. To tackle VBE large demand problems, a number of innovative solutions have been proposed. Berman and Bruneau [7] have employed the light-gauge steel plate for infill panels and epoxy material rather than welding so as to connect the infill to the boundary frame element. This new material eliminates the need for a thicker plate for proper welding, which

dramatically augments over-strength demand on the vertical boundary element. Vian and Bruneau [9] placed strategic holes in the infill panels and simultaneously used low yield point steels for the infill panel and reduced beam sections at beam-to-column connections for the boundary element. Baftechi and Zandi [10] used almost pure aluminum for the infill plate for the same reason as using low yield point steel in previous researches. Hitaka and Matsui [11] introduced the steel plate shear wall with vertical slits. In this system, the load carrying mechanism changes from tension field action to series of flexural links. Li et al. [12] installed some pin-ended horizontal elements called restrainers along the height of the VBE in a SPSW. These compression elements diminish the demands on the vertical boundary element and improve the pinching behavior of the unstiffened infill plate. Dastfan [13], Zhao and Astane-Asl [14], Choi and Park [15] used various types of vertical boundary elements to create economical method to tolerate existing demands. Jahanpour et al. [16] used a new type of steel shear wall called “Semi-supported steel shear wall (SSSW)”. Separating the VBE (secondary column) from the original frame column (primary column) which carries gravity load allows the development of plastic hinges in the secondary column without causing concern about the stability of the

* Corresponding author at: K. N. Toosi University of Technology, Civil Engineering Department, No. 1346, Vali-Asr Street, P.O. Box. 15875-4416, 19697 Tehran, Iran.

E-mail address: fanaie@kntu.ac.ir (N. Fanaie).

<https://doi.org/10.1016/j.istruc.2021.02.003>

Received 16 September 2020; Received in revised form 6 January 2021; Accepted 3 February 2021
 2352-0124/© 2021 Institution of Structural Engineers. Published by Elsevier Ltd. All rights reserved.

whole structure. Therefore, it leads to size reduction of the primary columns. A number of researchers [17–19] used reinforced concrete panel as a sandwich restrainer plate to eliminate or postpone web plate buckling and as a result load carrying mechanism changes from tension field action to pure shear. Guo et al. and Choi and Park [20,21] merely connected infill panels to the frame beam and exempted the vertical boundary element from experiencing large lateral forces. In what follows, this idea was comprehensively investigated by Qian and Astane-Asl [22]. Detaching web plate from connecting to VBE has above-mentioned advantage. However, it has some disadvantages like losing VBE ability in mobilizing web plate shear strength. Furthermore, out of plane displacement at the vertical free edges adjacent to VBE disturbing web plate from appropriate ductile behavior which forced attaching thick stiffener to eliminate out of plane deformation in this area [20,21]. To tackle this problem, partial length connected web plate to boundary element steel shear wall was introduced to compromise between this advantage and disadvantages. Wei et al. [23–26] introduced the partially connected buckling-restrained steel plate shear wall. In this system, half the height/width of the infill panel was covered by the precast RC restrainer not connected to the surrounding boundary elements.

Paslar et al. [27] evaluated the structural performance of the partially connected infill plates steel shear walls with various commonly used interconnections types compared to the corresponding conventional fully connected infill plate systems by establishing computational models. According to their research, systems with partial infill plate interconnection in middle height of VBE revealed a desirable structural behavior. Furthermore, with connectivity ratios of 80% in this type of infill-VBE interconnection, similar structural performance compared to the conventional system with the steel plate shear wall fully connected infill plates were observed.

According to Paslar et al. research, the purpose which led authors to carry out this investigation is to propose an innovative general analytical method of analysis and design of steel plate shear wall with lack of connection at the middle height of VBE based on numerical and experimental evidence.

The stages of this research include the explanation of the idea of not connecting the infill plate to middle height of VBE, validating experiment program and finite element modeling to prove the formation of parallel tension strips in web plate and developing governing equations to analyze the system.

2. Explanation of the idea of partial connection of infill to VBE

To better describing the idea of partial connection of infill to VBE, the following simplifications are considered. A single-story shear wall, with pin connections of the boundary elements to each other and VBE to the base, is considered as shown in Fig. 1. Fig. 2 shows the analytical model developed by Berman and Bruneau [28] (Considering the VBEs to act as a continuous member over a series of supports (HBEs) spaced at story height) a concentrated axial force component caused by horizontal boundary element (HBE) shear force and distributed loading due to the formation of a diagonal tension field in the infill plate are applied to VBE. This distributed load occurs at angle α from the vertical axis, with an intensity of $R_y F_y t_w$ (where R_y is the ratio of mean to nominal yield stress of the web plate, F_y is the web plate yield stress and t_w is the infill plate thickness).

This distributed loading can be decomposed to horizontal and vertical components acting along the VBE as shown in Fig. 2b. and c. These two components create bending and axial force in the VBE, respectively.

The infill plate is taken to be partially connected to the VBE, as shown in Fig. 3 and the h_{nc} (nc = not connected) length of the central part of the infill plate is not connected to VBE where h = distance between HBE centerlines, L = distance between VBE centerlines and NCR is the not connected length ratio ($NCR = h_{nc} / h$). Assuming that the inclination angle of the tension field is constant, the analytical model of the VBE of the shear wall for the horizontal component of the tension

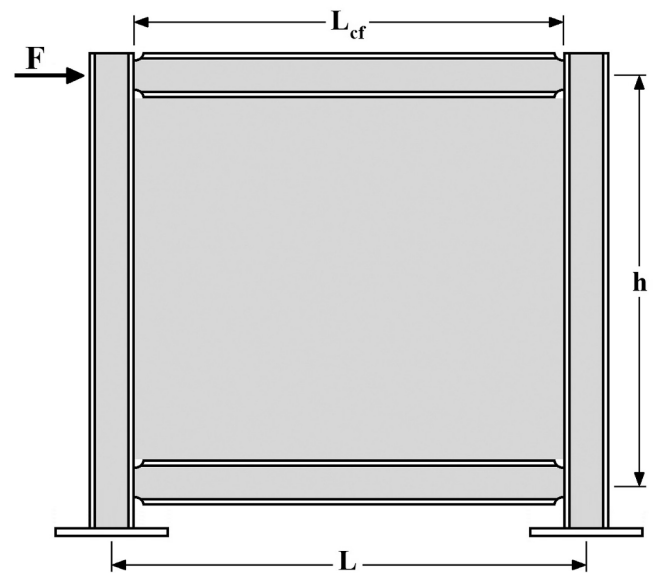


Fig. 1. Single story shear wall with pin connection of the boundary elements to each other and VBE to the base.

field, shown in Fig. 3, will be as illustrated in Fig. 4. As it can be seen the aim of this idea is to transfer heavy distributed load, due to tension field formation at mid span of VBE, close to the support in order to reduce flexure and stiffness demand on the vertical boundary elements.

Since the geometry introduced for the shear wall with partial length connection of infill plate to vertical boundary element is different from that of the conventional shear walls, the equations and concepts developed on the basis of previous geometry for the analysis and design of this system should be reconsidered. The most significant equations are as follows:

- 1) Panel shear strength
- 2) Inclination angle of tension field action
- 3) Minimum VBE stiffness requirement

Since the formation of parallel tension strips in the web plate is by far the most important assumption in deriving the specified steel shear wall governing equations. This assumption is the first to be validated using experimental and numerical evidence. It is worth mentioning that specific assumptions are provided to obtain each of the governing equations separately in its related section.

3. Validating program to prove the formation of parallel tension strips in web plate

In this survey according to the hypotheses of thin infill plate (not tolerating the compression stresses by the infill plate), sufficient stiffness of the boundary elements (a hypothesis which is going to be investigated later) and low not connected length ratio (which leads to venial deviation in tension strips inclination), it can be assumed that the tension strips are formed parallel to each other and with the same stress level. Despite the fact that at the onset of the tension field formation, the maximum stress in an infill panel may be significantly greater than the average caused by VBE flexibility and stress concentration at the initiating point of discontinuity, this difference could decrease with greater story drifts, provided that the boundary frame members are able to allow infill panel stress redistribution after the first yielding of tension diagonal strips.

To verify the above-mentioned assumption (formation of parallel tension strips in web plate), experimental and numerical survey programs have been organized considering various not connected length ratios.

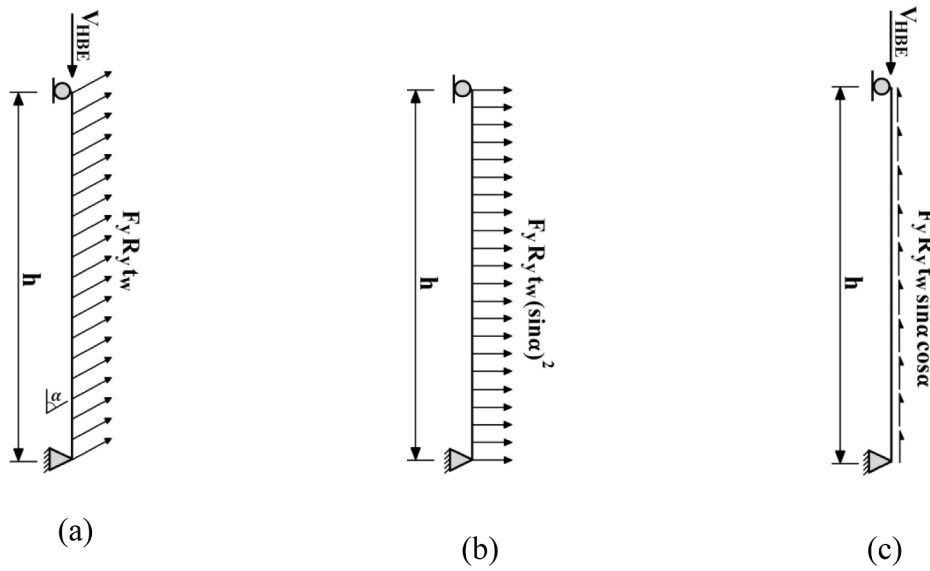


Fig. 2. Analytical model of VBE; (a) VBE free body diagram; (b) Horizontal component of tension field, acting along the VBE; (c) Vertical component of tension field, acting along the VBE.

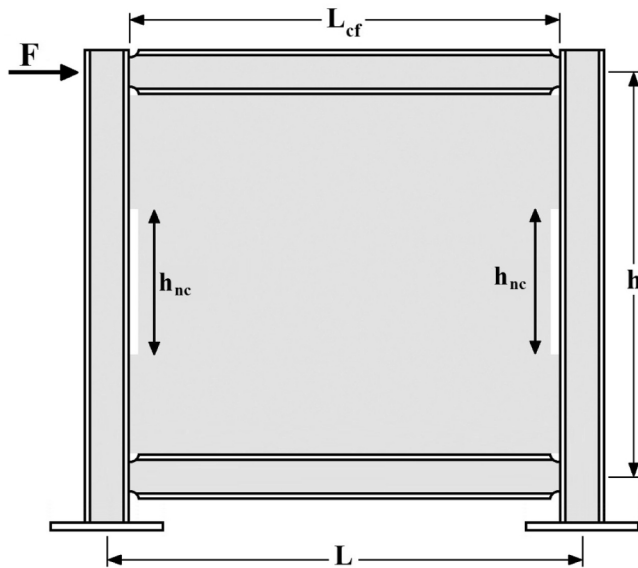


Fig. 3. Steel plate shear wall with partial length connection of infill plate to VBE.

3.1. Experimental program

3.1.1. Test specimens

Considering a broad range of not connected length ratio and the ease of experiments in a large number of experiments, an experimental study was conducted using four small-scale (a small one-tenth scale reusable testing assembly) specimens with different ratios of not connected infill plate to vertical boundary elements subjected to monotonic push-over loading.

Dimensional analysis and similitude were employed to determine the dimensions of small-scale specimens [29]. Parameters influencing the system behavior need to be determined in this method, namely, yield stress (F_y), not connected length ratio (NCR), height (h), clear distance between column internal face (L_{cf}), infill plate thickness (t_w), inclination angle of the tension field (α) and lateral shear strength of panel (V_n) were considered so as to determine the lateral strength of the wall induced by the infill plate. According to the Buckingham pi theorem, five

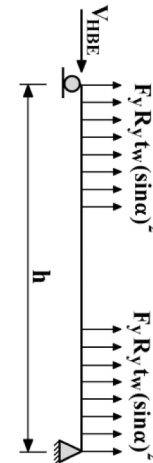


Fig. 4. Analytical model of VBE depicted in Fig. 3.

dimensionless parameters were obtained and presented in Table 1. The dimensions of the specimens were determined relative to the dimensions of the large-scale specimen according to Eq. (1) using the scale factor presented in Table 2.

Table 1
Pi Terms-Web Plate.

Variable	Dimension	Pi Term
Web plate thickness	t_w	$\Pi_1 = \frac{t_w}{L_{cf}}$
Tension field angle	α	$\Pi_2 = \alpha$
Yield stress	F_y	FL^{-2}
Clear distance between column internal faces	L_{cf}	L
Height	h	$\Pi_3 = \frac{h}{L_{cf}}$
Nominal shear strength	V_n	$\Pi_4 = \frac{V_n}{F_y L_{cf}^2}$
Not connected length ratio	NCR	$\Pi_5 = NCR$

Table 2
Scale factors used in the small-scale specimen design.

Variable	Test specimen	Large-scale specimen	Scale factors
Web plate thickness	0.3 mm	3 mm	0.1
Height	300 mm	3000 mm	0.1
Clear length of web panel between VBE internal faces	360 mm	3600 mm	0.1

$$\text{Target value} = SF \times (\text{Large scale value of the variable}) \quad (1)$$

The prototypes were designed based on presumed analytical model shown in Fig. 5. Boundary elements were designed considering conservative safety factor to ensure elastic behavior during the experiment. Angle of tension field inclination was considered equal to 45°. It should be noted that Gravity loads were not simulated since the reduction in VBE flexural stiffness resulting from increased axial load is negligible for most SPSW VBEs because these members are typically very stocky beam columns.

Because this experimental study aims to investigate the quality of tension field formation in the infill plate of shear wall, the horizontal and vertical boundary elements were selected with strength and stiffness more than those required (practically rigid elements) to avoid unnecessary computational complexities.

After the dimensions of the small-scale specimens are determined with conservative assumptions, high-strength boundary elements were considered for the wall. Owing to the overdesign of boundary elements as well as the presence of pinned joints, these elements remained completely elastic during the experiments (reusable boundary elements).

Web plate was sandwiched by each side of boundary elements through slip-critical bolted connections. To prevent the frame action from getting involved in the lateral strength of the wall, the connections of boundary elements to each other and to the supports were modeled as nearly ideal pinned joints with zero lateral strength. The detailed dimensions of specimens made according to above-mentioned considerations mounted on a strong thick plate are shown in Fig. 6.

Table 3 presents specimen codes according to the percentage of not connected infill plate connection to vertical boundary elements.

As an example, test setup of specimen with 10% not connected length ratio (S1) is shown in Fig. 7.

3.1.2. Materials

Mild structural steel (ST37) was employed for boundary elements. A very thin plate (with a thickness of 0.03 cm) was used for the infill plate in the shear wall with the mechanical specifications determined by the tension coupon test to evaluate the isotropic behavior of steel in two orthogonal directions (longitudinal and transversal directions) of the plate as presented in Table 4. Given the little difference between the yield stresses in both directions presented in Table 4, an average yield stress was considered in the calculations. Fig. 8 shows the stress-strain diagram of the infill plate steel in two orthogonal directions parallel to the horizontal and vertical boundary elements with corresponding coupon test specimens. To avoid the slip between specimens the universal testing machine grip due to using very low thickness specimens, grip section of coupon test specimen was sandwiched by sand paper with adhesive epoxy material so as to provide sufficient engagement.

3.1.3. Instrumentation

The instrumentations utilized to monitor the kinematic parameters (load and displacement) during the test are illustrated in Figs. 6 and 7. A linear variable displacement transducer was utilized at the right-hand side of top HBE of the specimen to measure the story displacement. To determine the magnitude of the applied force to the test specimen, one load cell transducer was placed between the actuator and left-hand side of top HBE of the specimen. Monotonic push-over loading was implemented by applying a lateral displacement in the middle level of the left-hand side of top HBE of the specimen through screw actuator and the displacement was measured on the right-hand side. In addition, a data acquisition system is used to collect the data from the LVDT and loadcell.

3.1.4. Test results and discussion

Fig. 9 qualitatively shows the formation of the tension field in four specimens. As it is obviously observed, the tension field is formed in all

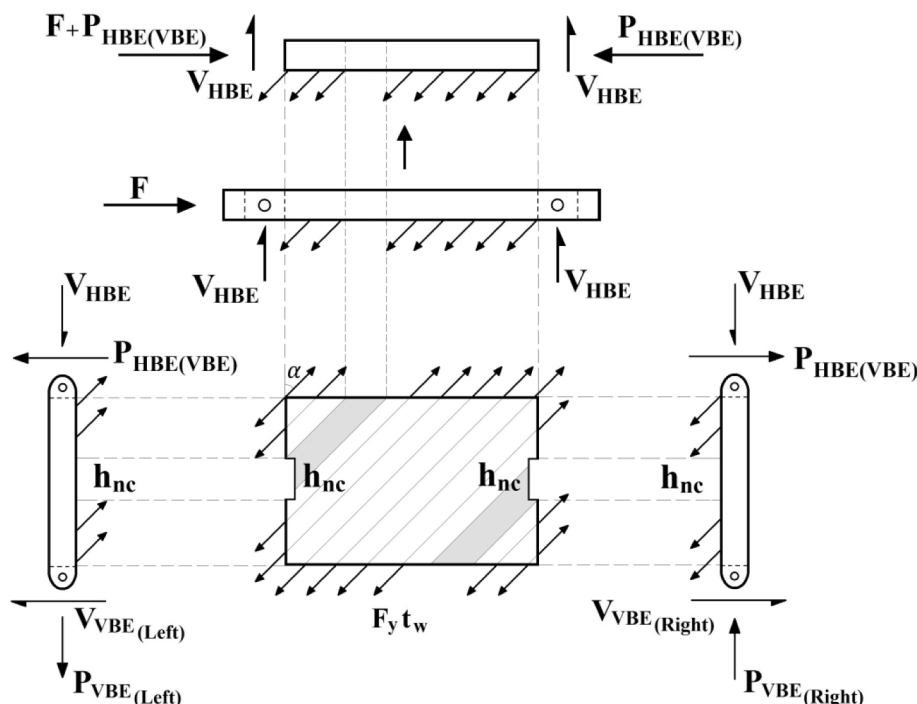


Fig. 5. Assumed analytical model of prototype.

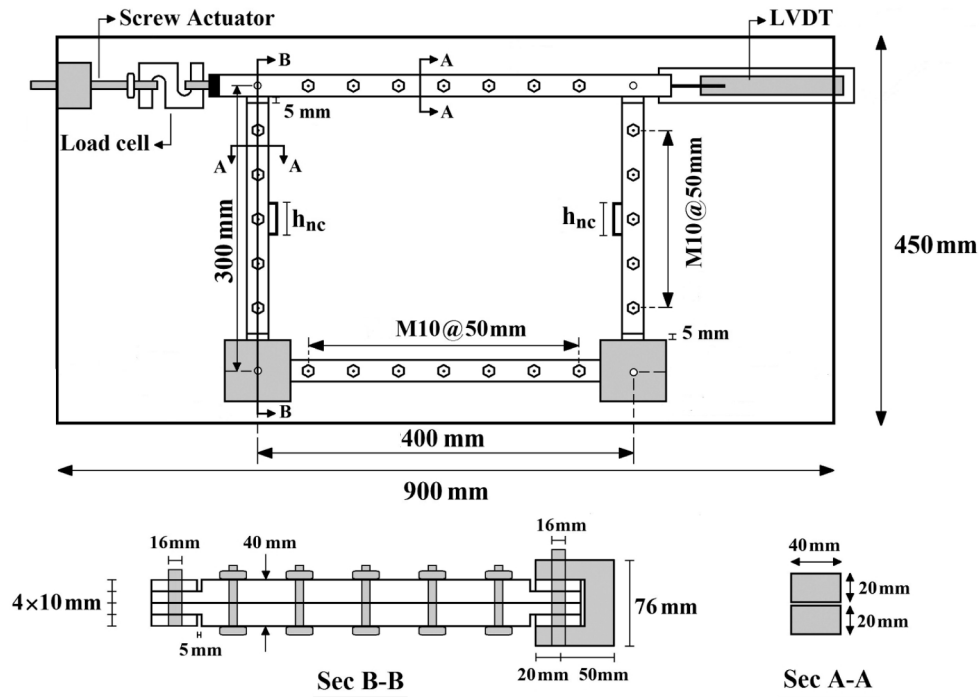


Fig. 6. Overall dimensions of small-scale test specimens.

Table 3
Specimen codes according to the not connected length ratio.

Specimen number	Not connected length ratio (NCR)	Code
1	0% (0cm)	S1
2	10% (3cm)	S2
3	20% (6cm)	S3
4	30% (9cm)	S3

four specimens in the form of relatively parallel strips. Therefore, the formation of parallel tension strips in the infill plate of the steel shear wall with partial length connection to vertical boundary elements was experimentally corroborated (at first based on qualitatively evident).

Fig. 10 separates web plate into two parts which is defined here by central zone (CE) and corner zone (CO). As it is obviously observed, the dominant share of web plate belongs to central zone and the other share belongs to corner zone. Increasing the not connected length ratio leads to tension field inclination deviation between two parts.

It should be noted that:

Increasing in not connected length causes the deviation of inclination angle in the circle zone (CO) as depicted in Fig. 11. This deviation in a partially connected infill plate occurs due to the ability of corner strips to save lesser amount of strain energy compared to the full connected infill plate against the constant external load. This event occurs by the formation of strips at the corners which are more horizontal compared to average strip inclination through the entire web plate. This leads to mobilizing more local stiffness and more load carrying capacity. This phenomenon leads to lower decreasing in ultimate strength in lower

Table 4
Results of coupon tests.

Direction	Yield stress (MPa)	Ultimate stress (MPa)	Strain at fracture (%)
Horizontal	323.5	339	7.2
Vertical	333.1	371.2	11.1
Average	328.3		



Fig. 7. Small-scale specimen test setup (NCR = 10%).

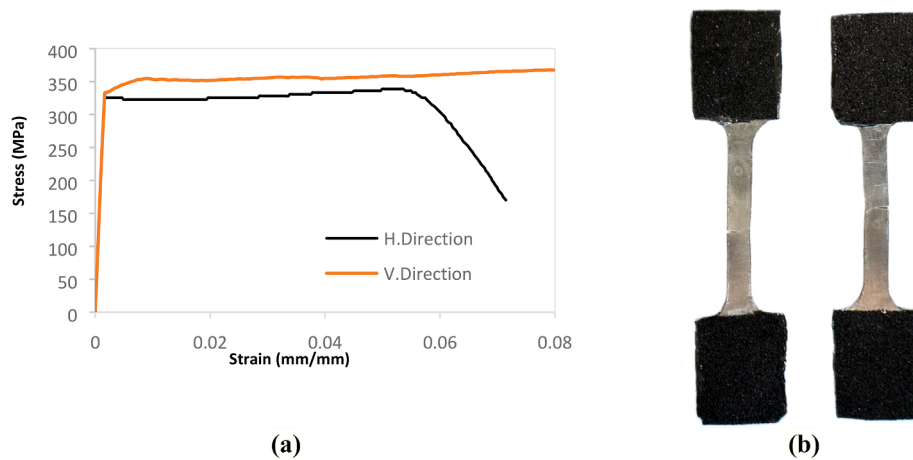


Fig. 8. (a) stress–strain diagram of the infill plate steel in two orthogonal directions, (b) corresponding coupon test specimens.

amount of not connected length ratio in comparison with fully connected conventional steel shear wall mentioned in Paslar et al. [27] study. The other merit of this phenomenon is to decrease in flexural demand on HBE by neutralizing of vertical component of tensile field action which acted on this element in upper and lower story. But this phenomenon increases the potential of web plate tearing close to the not connected part which is due to balance need (establishments of equilibrium). Lack of connection forced web plate to experience extra nonlinear deformation (undergo strain hardening region) for this purpose. Therefore, to achieve ductile response, ductile web plate material without sharp corner cutting in not connected part is needed.

3.2. Numerical program

3.2.1. Finite element model

To better explain the quality of tension field formation in the presence of infill plate with lack of connection in middle height of VBE, a supplementary 3D numerical parametric study was performed using commercial finite element software Abaqus 2016 and not connected length ratio of the infill plates is utilized as a variable for parametric study.

The web was modeled by S4R shell element which is a quadrilateral shell element with 4 nodes (linear shape function) and reduced numbers of Gaussian integration points (1 point). The element has six degrees of freedom (3 translational and 3 rotational DOFs) at each node of elements and considers both membrane and bending behaviors. This kind of element is suitable for both material and geometric nonlinearity considerations [30]. A set of mesh sensitivity analyses were conducted and by considering a trade-off between computational cost and desired accuracy in conformance with experimental results, 5 mm refined mesh was chosen for infill plate.

Boundary elements were modeled using B31 shear deformable beam elements so as to reduce unnecessary computational costs. The web plate was attached to the surrounding boundary elements by the “tie” constraint. The effect of this approximation on the analysis results was found to be small and can be ignored, Driver et al. [31]. Connections of boundary elements to each other were modeled as pinned joints by “joint + rotation” connector element. Also, connections of boundary

element to the supports were modeled as a hinge and top HBE was prevented from out-of-plane displacement.

A bilinear curve was used to describe the stress–strain diagram of infill steel plate. This bilinear stress–strain diagram extends from the origin to an average value of the transverse and longitudinal direction yield stress (using pairs of true stress (Cauchy stress) and true strain, σ_{true} and ϵ_{true} , respectively) and after yield stress the hardening behavior is considered and the stress is assumed to linearly increase until the plastic strain reach up to approximate 0.05. Isotropic hardening law (i. e., an expansion of the yield surface while undergoing plastic strains) is generally true for uniaxial stress state. Therefore, because of the nearly uniaxial stress state experience in web plate and elastic stress state of frame boundary element due to applied monotonic loading, isotropic hardening law was used for web plate material.

Solution strategies for physical problems via nonlinear FEM are divided into two categories, implicit and explicit methods. The implicit method solution is used for static and quasi-static analyses [30]. Therefore, due to the quasi-static type of SPSWs monotonic loading, for nonlinear analysis of FE models, an implicit method (quasi-static) is used. In all simulations implicit dynamic analysis was employed. Because of numerical instability and convergence problems due to buckling analysis, dynamic solver used instead of static one, and the load was gradually applied to minimize the dynamic effect. To monitor dynamic effect, ratio of kinetic energy to total energy was checked in all analyses and was observed to be negligible. A good accordance to experimental analysis was observed which corroborates that the dynamic effect was insignificant. The Newton-Raphson method is used to solve the nonlinear equations of FE models.

3.2.2. Imperfection

The initial shape of each infill panels was not recorded prior to testing, although because of accurate design and construction of small-scale test specimens insignificant out-of-plane deformations deviation from perfect flatness were visually observed. However, these negligible imperfections finally helped precipitate the global panel buckling and, therefore, need to be considered in the FE analysis of the specimens. To account for the initial imperfections, an eigenvalue buckling analysis was performed on the perfect structure, i.e. undeformed model prior to

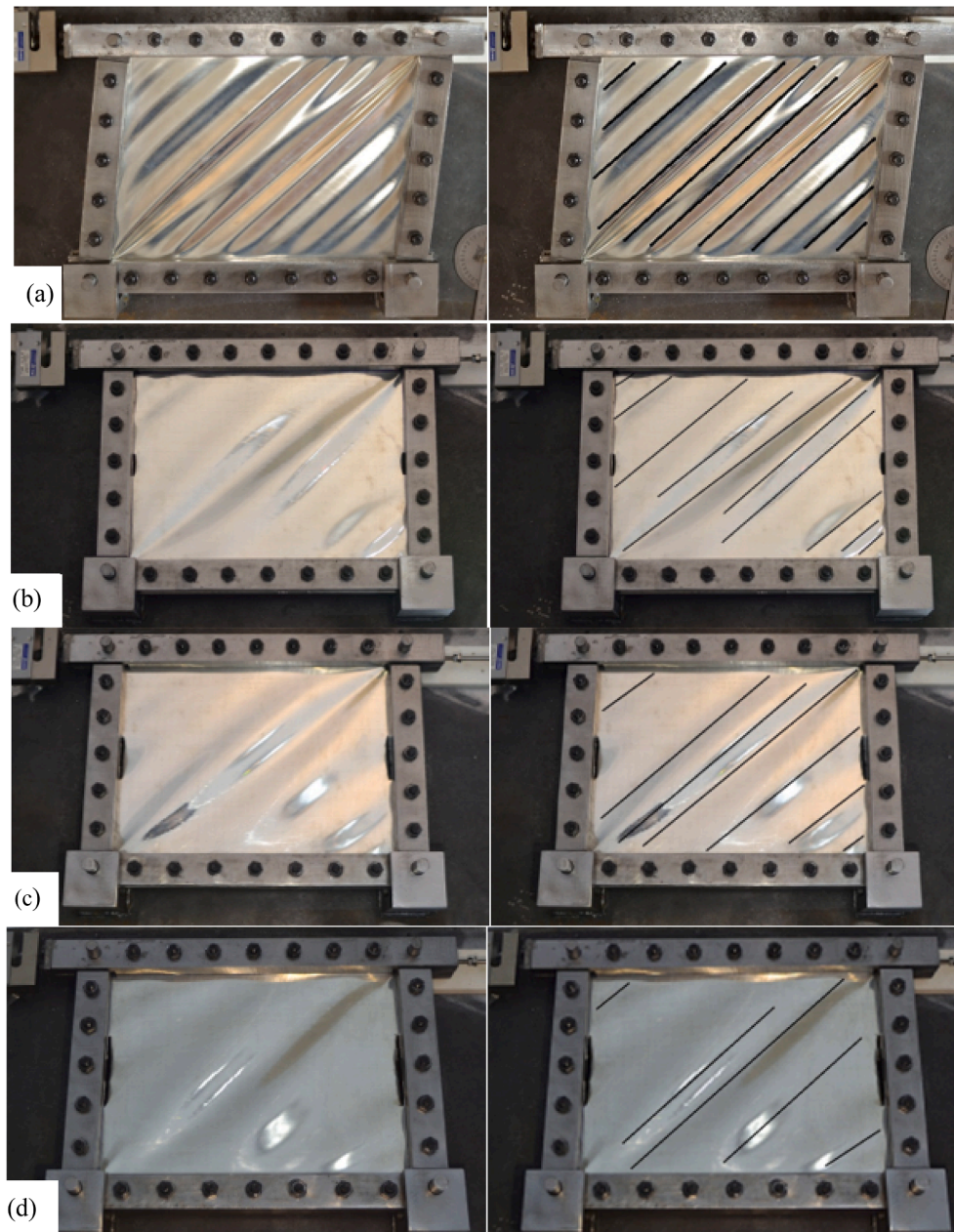


Fig. 9. Formation of nearly parallel tension field strip in four small-scale test specimens a) S1; b) S2; c) S3; d) S4 – (in order to visually observe the tension field inclination, a series of sloped guide line were drawn on the photograph of the test specimens.)

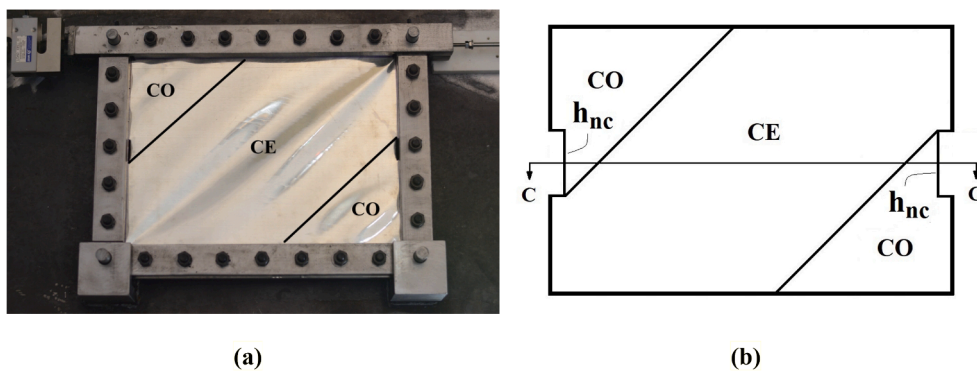


Fig. 10. Separation of web plate into two parts; (a) S2 specimen as an example, (b) schematic shape.

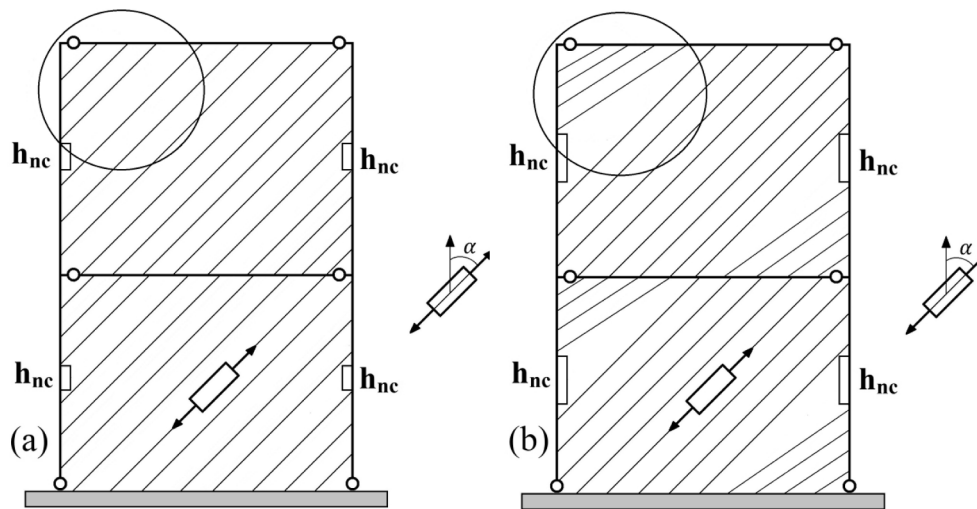


Fig. 11. Deviation in tension strips inclination due to the increase in not connected length ratio (a) presume web plate tension strips inclination in this research with respect to small not connected length ratio; (b) actual tension strips inclination due to increasing in not connected length ratio.

applying push-over load, to determine the first thirty panel buckling mode shapes. Finally, 23th, 21th, 22th and 9th buckling mode shapes were selected for S1 to S4 FE models, respectively. These desired mode shapes were selected firstly in qualitative manner based on almost the same number of buckling wave created in the web plate of FE models corresponding to test specimens and finally were selected so that they represent better match compared to the infill panel load-deformation behavior due to push-over loading.

The buckling mode shapes were scaled to have 1 mm amplitude for each panel, and were added to the perfect model using the imperfection command. Then displacement-controlled monotonic loading was applied to the top HBE in left to right direction.

3.2.3. Results and discussion

The finite element analysis model in comparison with deformed test specimens are shown in Fig. 12.

Based on the above-mentioned description, Fig. 12. (d) shows somewhat deviation in tension field inclination in corner zone rather than central zone.

Fig. 13. Illustrated the variation of web plate principal stress acting across the HBE with respect to percent of interstorey drift ratio. As it is observed, principal stress acting across the HBE length which is due to the deviation of inclination angle in the circle zone (CO) depicted in Fig. 11. This figure also shows that the low not connected infill plate ratio has no significant effect on the HBE tangential load demand due to web plate tension field formation. Also, nearly uniform shear stress formed across HBE length except lack of connection affected zone which prove formation of same stress level tension strip in web plate.

Fig. 14 illustrated shear load intensity acting across the HBE. Comparison between this figure and Fig. 13. shows that the uniformity of distributed shear load intensity was less affected by lack of connection to VBE rather than principal stress as a result prove the formation of more horizontal strip at the corner zone compared to average strip inclination through the entire web plate which compensate the decrease in principal stress by new inclination which leads to mobilizing more local stiffness and more load carrying capacity.

Based on the aforementioned experimental and numerical study, parallelism in tension field strip inclination can be used across the entire infill plate in case, not connected length ratio is less than 30%. The same acceptable stress level strip formation occurred for this numerical model which is quantitatively investigated subsequently.

4. Panel shear strength

In the conventional steel shear wall, shear strength of the infill plate (with the limit state of shear yielding) is determined in accordance with Berman and Bruneau’s [32] proposed equation derived from the plastic analysis of the strip model, which is an accepted (AISC 341-16 [33]) model for the representation of steel shear walls as follows:

$$V = 0.5R_y F_y L_{cf} t_w \sin(2\alpha) \tag{2}$$

where L_{cf} = clear distance between column flanges, as shown in Fig. 1.

According to the previous part assumptions and the details shown in Fig. 15, it can be concluded that the modified infill plate shear strength (V_m) caused by an intentional lack of connection is equal to the horizontal component of tension field stress (σ_{12}) multiplied by the effective cross-sectional area of infill plate tolerating the stress ($(L_{cf} - L_{NEff}) \times t_w$). Where $L_{NEff} \times t_w$ is the ineffective cross-sectional area of infill plate.

With respect to the equilibrium equations in horizontal and vertical directions, the amount of stress can be determined as shown in Fig. 15. It should be noted that in these equations, σ is the expected yield stress of infill plate ($R_y F_y$).

$$\sigma_{11} = \sigma \cos^2(\alpha) \tag{3}$$

$$\sigma_{12} = \sigma \sin(\alpha) \cos(\alpha) = 0.5\sigma \sin(2\alpha) \tag{4}$$

$$\sigma_{22} = \sigma \sin^2(\alpha) \tag{5}$$

$$\sigma_{21} = \sigma \sin(\alpha) \cos(\alpha) = 0.5\sigma \sin(2\alpha) \tag{6}$$

According to the above-mentioned equations and assumptions, the panel shear strength of steel shear wall with the partial length

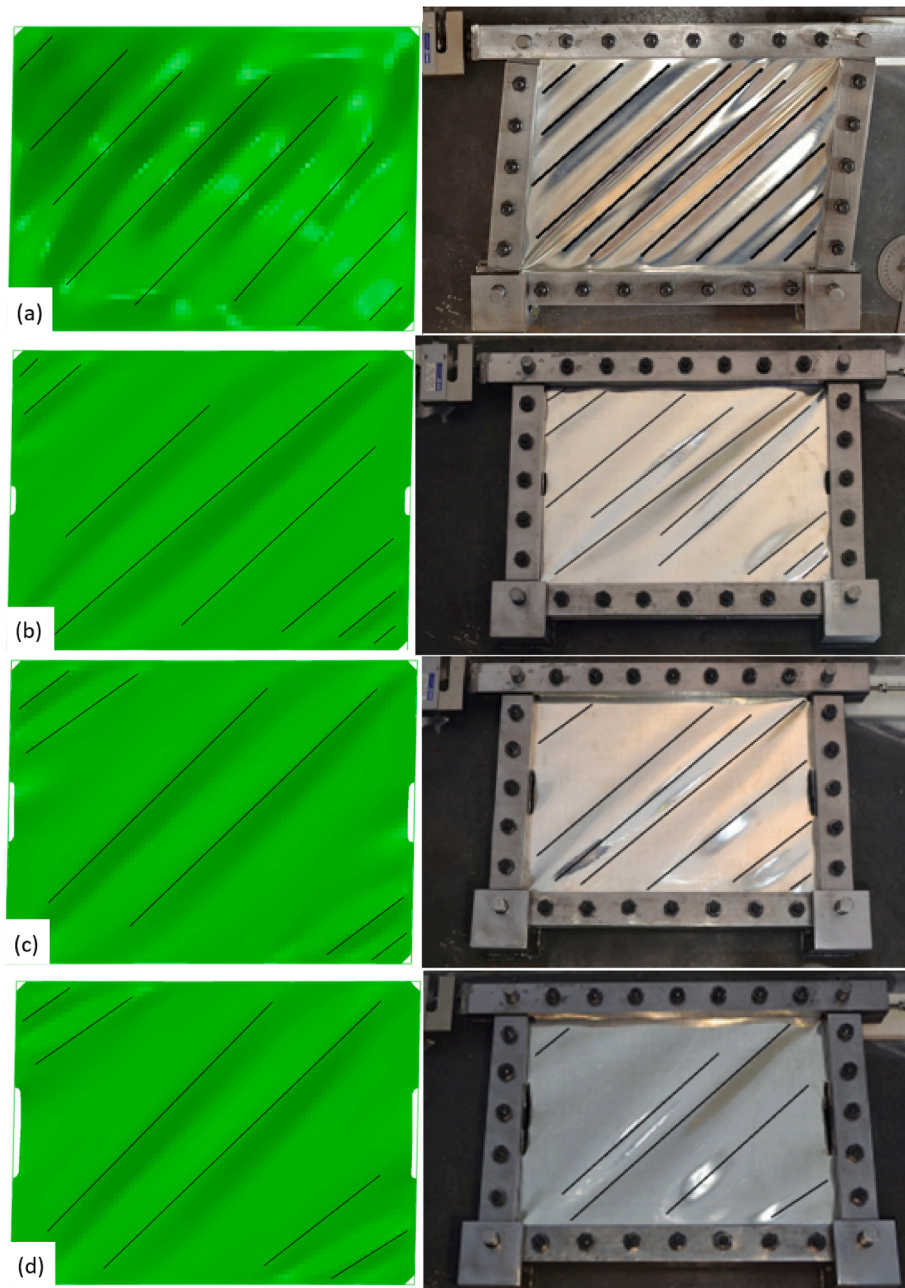


Fig. 12. Inclination of tension strip in finite-element model (2% Drift Ratio) in comparison with deformed small-scale test specimens (a) S1; b) S2; c) S3; d) S4 – (in order to visually observe the tension field inclination, a series of sloped guide line were drawn on the photograph of the test specimens-crest of the buckle wave).

connection of the infill plate to vertical boundary element can be calculated using the following equation.

$$V_m = 0.5R_y F_y (L_{cf} - L_{NEff}) t_w \sin(2\alpha) \tag{7}$$

Based on the geometric calculations (Fig. 15.), the following equation exists between L_{NEff} and h_{nc} .

$$L_{NEff} = h_{nc} \tan(\alpha) \tag{8}$$

As seen, modified infill plate shear strength (V_m) linearly decreases by increasing in not connected length ratio ($NCR = h_{nc}/h$).

Fig. 16 illustrates nine pre-selected node locations through path which was defined as the representative of web plate central zone for all the pre described finite element Models. Table 5 depicts the coefficient of variation of principal stress inclination at the nine pre-selected finite element model with respect to percent of interstory drift ratio (a

previous study by Webster et al. [34] shows that the tension field angle varies with the story drift in conventional SPSW). As it can be seen, the coefficient of variation value is close to zero which quantitatively guarantees the formation of parallel tension field in central zone of web plate which is utilized to determine panel shear strength in the next step.

Fig. 17 depicts the distributed shear load intensity due to tension field stress ($\sigma_{12} \times t_w = \text{shear flow}$) along the web plate cross section cut. (section C–C in Fig. 10.) As it clearly can be seen, almost uniformly distributed load were mobilized along the effective length ($L_{cf} - L_{NEff}$) of this section. So Fig. 17. validates the Eq. (7). As it is observed, distributed shear load mobilizes in effective width of web plate central part (plateau-shaped distribution).

5. Tension field inclination angle

A derivation for the angle of inclination of the tension field within

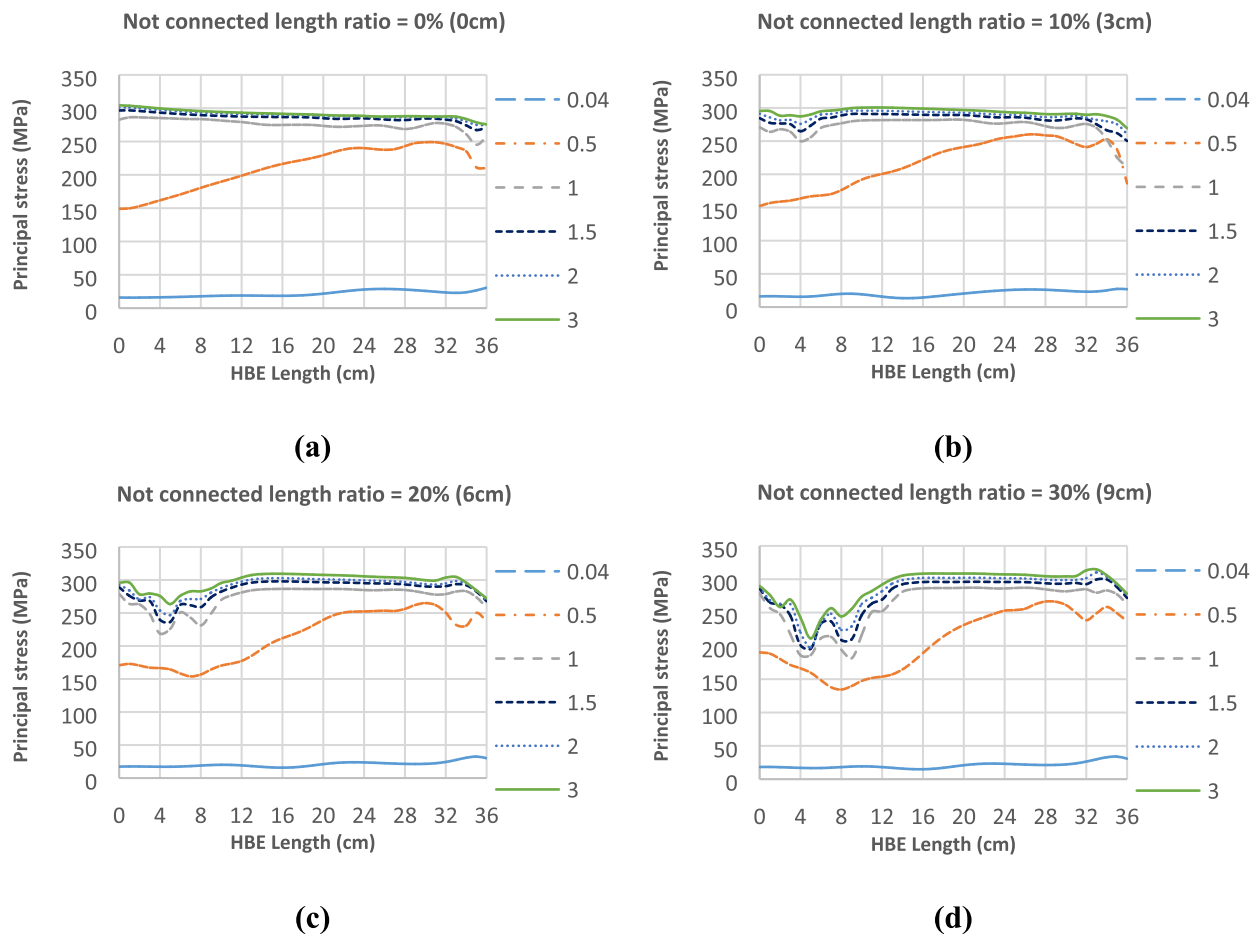


Fig. 13. Principal stress value due to tension field stress along the HBE length with respect to percent of interstory drift ratio.

the infill plate of an unstiffened shear wall subjected to transverse loading was first presented by Thorburn and Kulak in 1982 [35] using least work method. The work expression derived by these researchers merely includes stored strain energy caused by axial forces within the system considering an assumed uniform tension field within the plate. It was considered that the contribution of column bending strain energy should be included in the total stored strain energy, Timler and Kulak in 1984 [36]. It is due to the fact that the columns have an unbalanced force acting on one flange face as a result of the tension field causing the columns to be subjected to bending.

In this research project in order to determine angle of tension field inclination, ‘the least work principle’ employed by Timler and Kulak was used to determine the angle of tension field inclination in conventional steel shear walls. It is assumed that the strain energy is stored in the infill plate as membrane, in the horizontal boundary elements as axial and in vertical boundary elements as axial and flexural. Similar to Timler and Kulak study, the following assumption were made in the modeling to simplify the formulation:

- Since the thin infill plate cannot tolerate compressive stresses, the web energy associated with the compressive forces perpendicular to the tension field was assumed to be inconsequential.
- According to the hypothesis of thin infill plate and sufficient stiffness of the boundary elements (the hypothesis is going to be investigated in next part), it can be assumed that the tension strips are formed with the same stress level and are parallel to each other.
- The infill plate is idealized to be connected to the centerlines of the framing members.

- Since the two adjacent story earthquakes induced shear action for usual load cases have minor differences, and the tension fields acting on an interior beam can be considered equal (see Fig. 18.). Therefore, vertical load transfer as a result of the shear within the web panel is only done through the columns.
- Summation of forces in the horizontal direction indicates the beam axial force. A further simplification is introduced because the applied lateral load which should be observed at the floor level is not included in the summation. Therefore, the resultant axial force in the beam is considered as constant at a value $V_{NC} (h - h_{nc}) \tan(\alpha) / (L - h_{nc} \tan(\alpha))$ (see Fig. 18) when in fact it has a linearly varying shape in a similar way.
- The column axial force will be considered as the simplified value of $V_{NC} / (2 \tan(\alpha))$ (see Fig. 18). Its true shape also varies linearly as the vertical components of the tension field force is applied along the length of the column.
- The bending effect of the horizontal component of the tension field force acting on the column will be determined by considering the column to act as a member with fixed support.
- The tension field inclination angle deviation caused by discontinuity of the infill plate to the vertical boundary elements connection, is neglected (an additional assumption considered in this study).

As a result, according to Fig. 18 the total strain energy is stored in one panel, which consists of two vertical boundary elements, a horizontal boundary element and an infill plate (web plate), displayed as follows.

$$W_{Total} = W_{Web} + W_{Beam} + W_{Column} \tag{9}$$

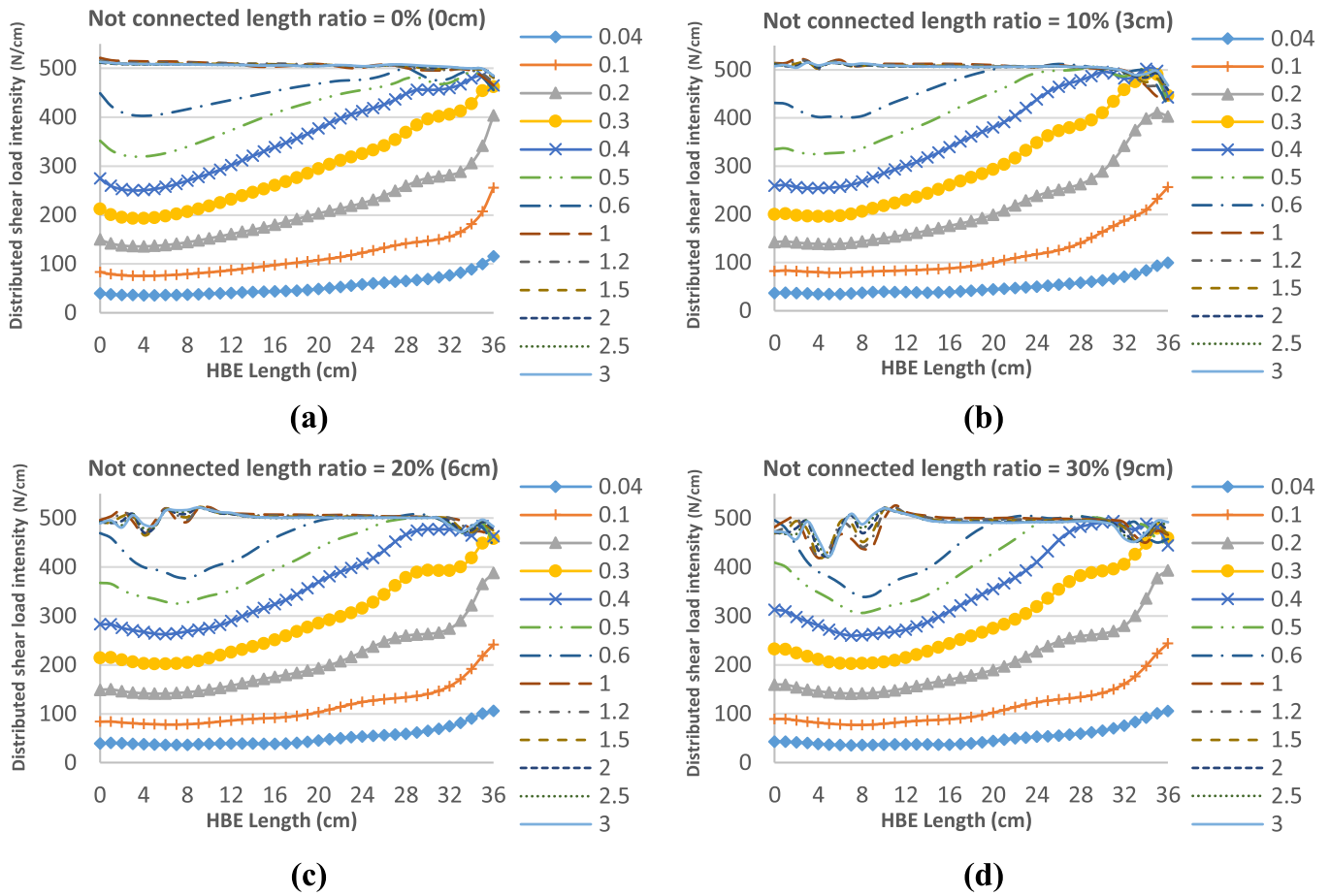


Fig. 14. Distributed shear load intensity due to tension field stress along the HBE length with respect to percent of interstory drift ratio.

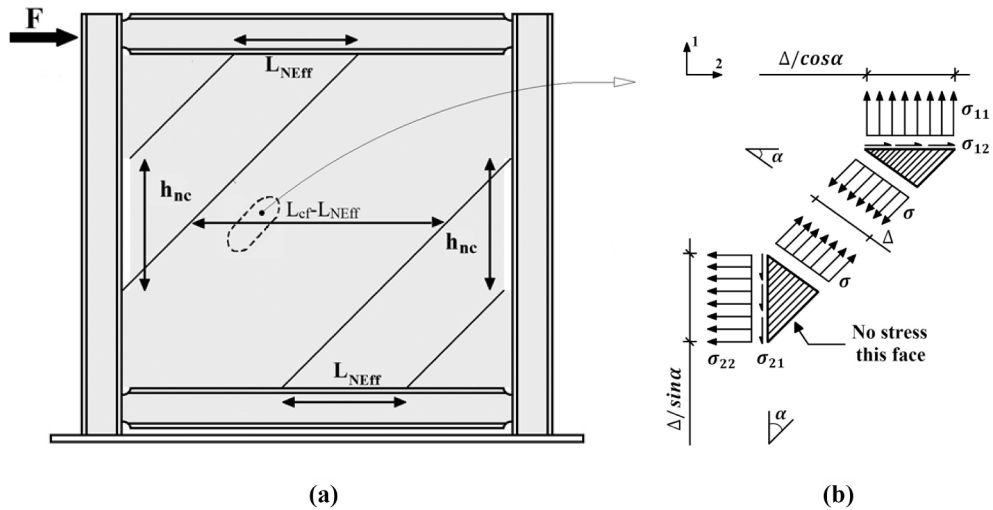


Fig. 15. Tension field stress details in partial length connection steel shear wall; (a) effective length of infill plate tolerating the stress ($L_{ef} = L_{NEFF}$), (b) decomposition of diagonal stress.

$$W_{Column} = W_{Axial} + W_{Bending} \tag{10}$$

It should be mentioned that the total shear V induced by lateral load is assumed to be merely withstood by the infill plate.

Where A_b = cross-sectional area of an HBE, A_c = cross-sectional area of a VBE and I_c = moments of inertia about an axis taken perpendicular to the plane of the web of VBE. The strain energy stored in infill plate

because of membrane force is as follows:

$$W_{Web-nc} = \int \frac{\sigma^2}{2E} dV \tag{11}$$

Based on Eq. (7), σ is calculated and presented as follows:

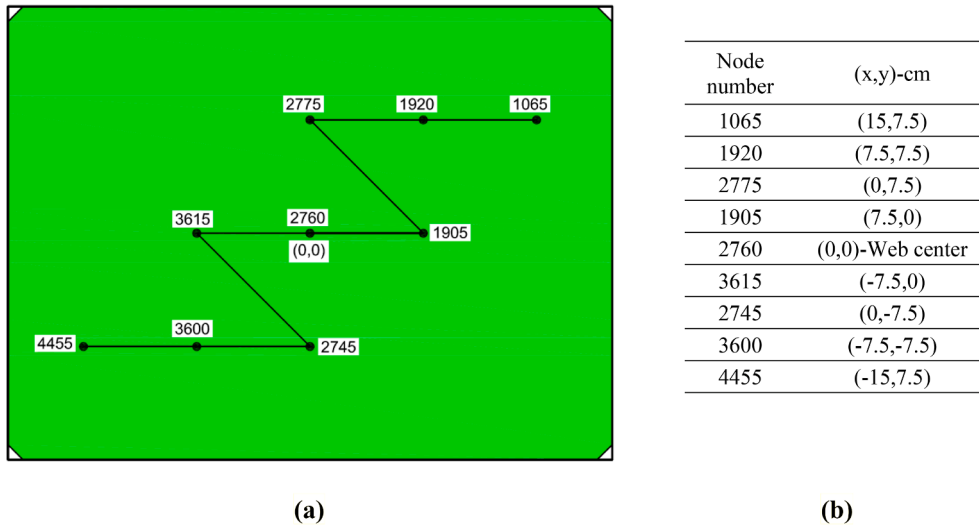


Fig. 16. Nine pre-selected node locations through path; (a) S1 model as a sample; (b) corresponding path coordinate.

Table 5
Coefficient of variation of principal stress inclination in web central zone with respect to percent of interstory drift ratio.

Drift Ratio	0.04	0.1	0.2	0.3	0.4	0.5	0.6	1	1.2	1.5	2	2.5	3
$h_{nc} = 0$	0.019	0.004	0.009	0.007	0.005	0.005	0.007	0.007	0.006	0.006	0.006	0.005	0.005
$h_{nc} = 3$	0.036	0.020	0.015	0.010	0.010	0.004	0.005	0.007	0.008	0.009	0.011	0.011	0.012
$h_{nc} = 6$	0.025	0.015	0.012	0.008	0.003	0.004	0.005	0.014	0.015	0.016	0.015	0.013	0.012
$h_{nc} = 9$	0.026	0.016	0.014	0.012	0.008	0.008	0.009	0.014	0.014	0.014	0.014	0.013	0.013

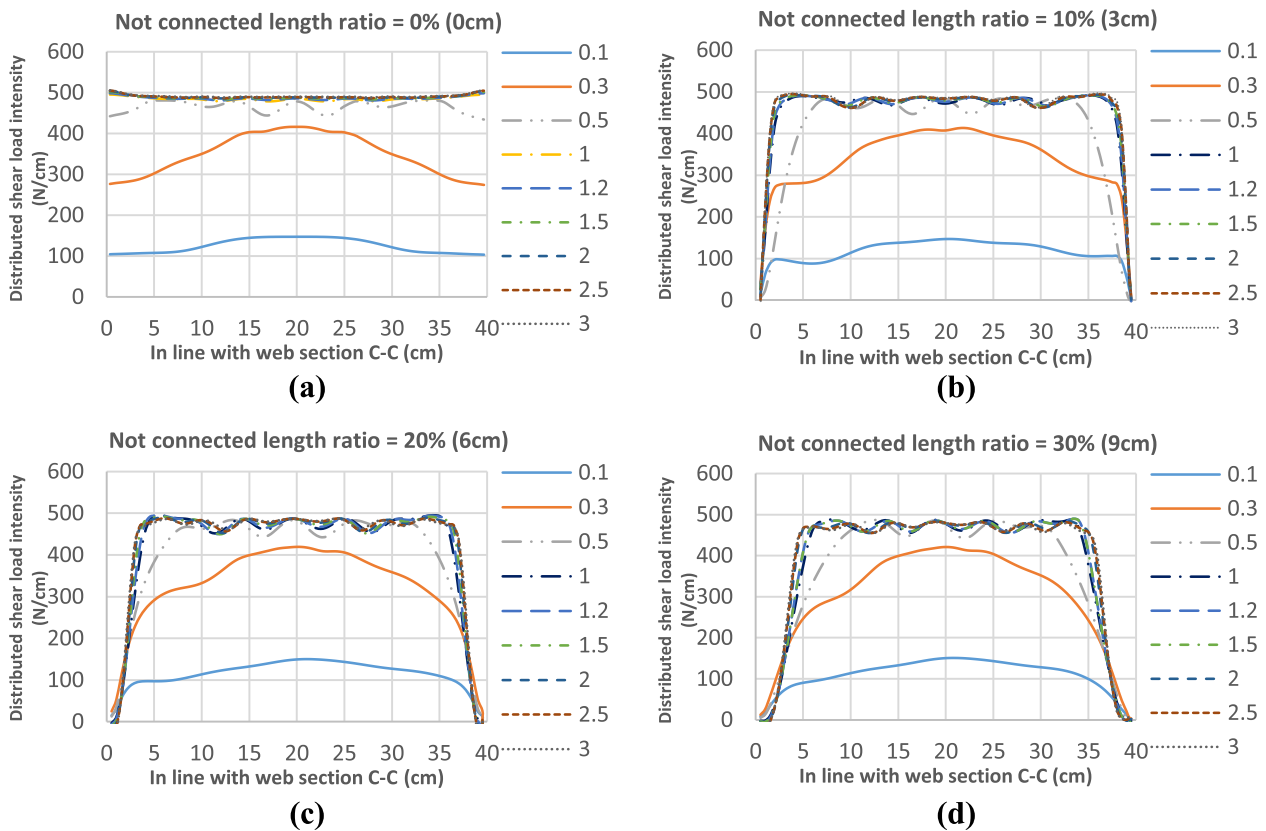


Fig. 17. Distributed shear load intensity due to tension field stress ($\sigma_{12} \times t_w$) along the web plate cross section cut (section C-C in Fig. 10.) with respect to percent of interstory drift ratio S1; b) S2; c) S3; d) S4 (plateau-shaped distribution).

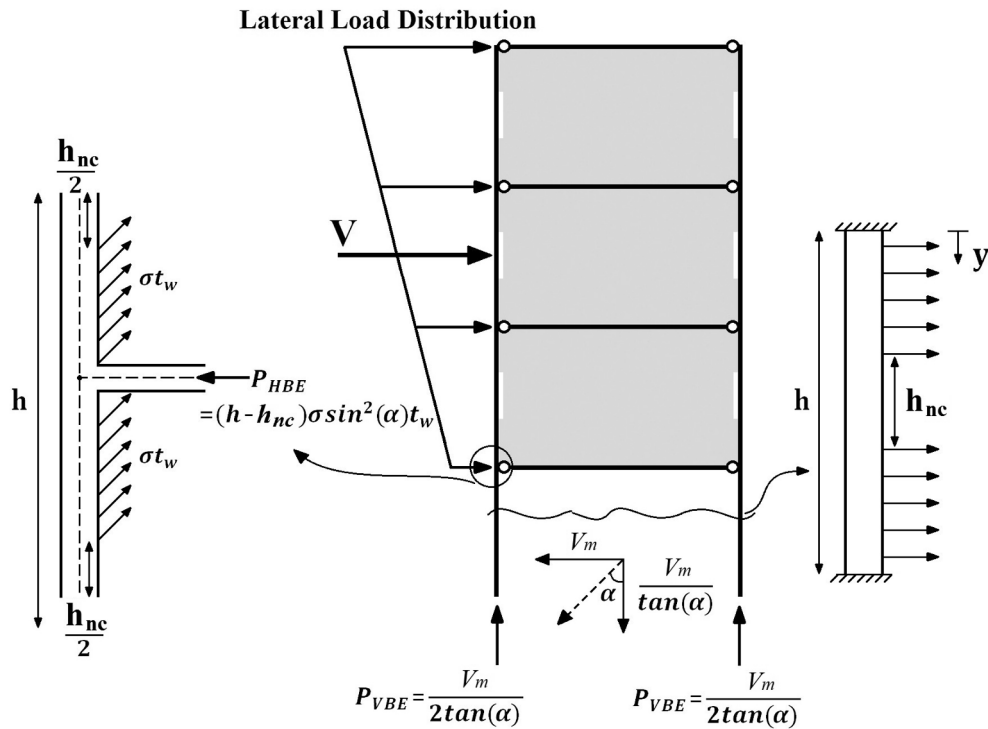


Fig. 18. Panel configuration used for strain energy calculation.

$$\sigma = \frac{V_m}{(L - h_{nc} \tan(\alpha)) \sin(\alpha) \cos(\alpha) t_w} \tag{12}$$

Where $V = h t_w (L - h_{nc} \tan(\alpha))$ is the effective volume of infill plate tolerating tension stress.

Finally, the stored strain energy in web plate is presented below:

$$W_{Web-nc} = \frac{V_m^2 h (1 + \tan^2(\alpha))^2}{2 E t_w (L - h_{nc} \tan(\alpha)) \tan^2(\alpha)} \tag{13}$$

The stored strain energy in HBE is as follows:

$$W_{Beam-NC} = \int_{x=0}^{x=L} \frac{P_{HBE}^2}{2 A_b E} dx \tag{14}$$

where P_{HBE} is defined outlined below:

$$P_{HBE} = (h - h_{nc}) \sigma \sin^2(\alpha) t_w = V_m \frac{(h - h_{nc})}{(L - h_{nc} \tan(\alpha))} \tan(\alpha) \tag{15}$$

Finally, the stored strain energy in HBE is as follows:

$$W_{Beam-NC} = \frac{V_m^2 ((h - h_{nc})^2 \tan^2(\alpha) L)}{2 (L - h_{nc} \tan(\alpha))^2 A_b E} \tag{16}$$

The stored strain energy due to axial force in VBE is as follows:

$$W_{C-nc(Axial)} = 2 \int_{y=0}^{y=h} \frac{P_{VBE}^2}{2 A_c E} dx \tag{17}$$

$$P_{VBE} = \frac{L \sigma \cos^2(\alpha) t_w}{2} = \frac{V_m}{2 \tan(\alpha)} \tag{18}$$

Finally, the stored strain energy in VBE due to axial force is as follows

$$W_{C-nc(Axial)} = \frac{V_m^2 h}{4 E A_c \tan^2(\alpha)} \tag{19}$$

VBE stored strain energy due to bending is as follows:

$$W_{C-nc(Bending)} = \int \frac{M^2(y)}{2 E I_c} dy \tag{20}$$

$$= 2 \left(\int_0^{\frac{h-h_{nc}}{2}} \frac{M^2(y)}{2 E I_c} dy + \int_{\frac{h-h_{nc}}{2}}^h \frac{M^2(y)}{2 E I_c} dy \right)$$

where $M(y)$ denotes bending moment of section in which y represents the vertical distance from the intersection of VBE and HBE as shown in Fig. 18. Finally, the stored strain energy in VBE due to bending moment is as follows:

$$W_{C-nc(Axial)} = \frac{4 \times V_m^2 \tan^2(\alpha)}{(L - h_{nc} \tan(\alpha))^2} \left(\int_0^{\frac{h-h_{nc}}{2}} \frac{\left(\frac{(h-h_{nc}) \cdot \left(2 h \frac{h_{nc}^2}{h} - h_{nc} - 12 y \right)}{24} + \frac{y^2}{2} \right)^2}{2 E I_c} dy + \int_{\frac{h-h_{nc}}{2}}^h \frac{\left(\frac{-(h-h_{nc})^3}{24 h} \right)^2}{2 E I_c} dy \right) = \frac{V_m^2 \tan^2(\alpha) (4h + 5h_{nc}) (h - h_{nc})^5}{2880 E I_c h (L - h_{nc} \tan(\alpha))^2} \tag{21}$$

The energy equation can now be formulated. In a typical panel, the energy within the frame consists of the contributions from the infill plate, one beam, and two columns. The internal work of the aforementioned components is individually evaluated and then are added so as to

$$IFh_{nc} = 0 \Rightarrow A = 0, B = 0, C = \left(\frac{2hL^2}{t_w} + \frac{2h^2L^2}{A_b} + \frac{h^5L}{180I_c} \right), D = 0, E = 0, F = 0, G = -\frac{2L^2h}{t_w} - \frac{hL^3}{A_c}$$

$$Eq.(26) : \left(\frac{2hL^2}{t_w} + \frac{2h^2L^2}{A_b} + \frac{h^5L}{180I_c} \right) \tan^4(\alpha) - \frac{2L^2h}{t_w} - \frac{hL^3}{A_c} = 0 \Rightarrow \tan^4(\alpha) = \frac{1 + \frac{t_wL}{2A_c}}{1 + t_w h \left(\frac{1}{A_b} + \frac{h^3}{360I_cL} \right)}$$
(27)

yield the total internal work which equals the stored total strain energy. The internal work done by the panel under a tension field stress is calculated as follows:

$$W_{Total} = \frac{V_m^2}{2E} \left(\frac{h(1 + \tan^2(\alpha))^2}{t_w(L - h_{nc} \tan(\alpha)) \tan^2(\alpha)} + \frac{((h - h_{nc})^2 \tan^2(\alpha)L)}{(L - h_{nc} \tan(\alpha))^2 A_b} + \frac{h}{2A_c \tan^2(\alpha)} + \frac{\tan^2(\alpha)(4h + 5h_{nc})(h - h_{nc})^5}{1440I_c h(L - h_{nc} \tan(\alpha))^2} \right)$$
(22)

According to the least work principle the critical value of α is obtained by minimizing the work done by differentiating with respect to α and equating the result to zero.

$$\frac{\partial W_{Total}}{\partial \alpha} = 0 \Rightarrow \frac{d}{d\alpha} \left(\frac{V_m^2}{2E} \left(\frac{h(1 + \tan^2(\alpha))^2}{t_w(L - h_{nc} \tan(\alpha)) \tan^2(\alpha)} + \frac{((h - h_{nc})^2 \tan^2(\alpha)L)}{(L - h_{nc} \tan(\alpha))^2 A_b} + \frac{h}{2A_c \tan^2(\alpha)} + \frac{\tan^2(\alpha)(4h + 5h_{nc})(h - h_{nc})^5}{1440I_c h(L - h_{nc} \tan(\alpha))^2} \right) \right) = 0$$
(23)

After deriving differentiated terms and manipulating them (presented in Eqs. (24) and (25)) into achieving a simplified equation, an equation of degree 6 (Eq. (26)) is obtained in terms of $\tan(\alpha)$ with constant coefficients.

$$+ \frac{(1 + \tan^2(\alpha))^2 h(-h_{nc} \tan^3(\alpha) + 2L \tan^2(\alpha) + 3h_{nc} \tan(\alpha) - 2L)}{(L - h_{nc} \tan(\alpha))^2 t_w \tan^3(\alpha)} + \frac{2(h - h_{nc})^2 \tan(\alpha) L^2 (1 + \tan^2(\alpha))}{(L - h_{nc} \tan(\alpha))^3 A_b} - \frac{h(1 + \tan^2(\alpha))}{A_c \tan^3(\alpha)}$$

$$+ \frac{(4h + 5h_{nc})(h - h_{nc})^5 \tan(\alpha)(1 + \tan^2(\alpha))L}{720I_c h(L - h_{nc} \tan(\alpha))^3} = 0$$
(24)

$$\frac{(1 + \tan^2(\alpha))h(-h_{nc} \tan^3(\alpha) + 2L \tan^2(\alpha) + 3h_{nc} \tan(\alpha) - 2L)(L - h_{nc} \tan(\alpha))}{t_w} + \frac{2(h - h_{nc})^2 \tan(\alpha)^4 L^2}{A_b} - \frac{h(L - h_{nc} \tan(\alpha))^3}{A_c} + \frac{(4h + 5h_{nc})(h - h_{nc})^5 \tan(\alpha)^4 L}{720I_c h} = 0$$
(25)

$$A \tan^6(\alpha) + B \tan^5(\alpha) + C \tan^4(\alpha) + D \tan^3(\alpha) + E \tan^2(\alpha) + F \tan(\alpha) + G = 0$$

$$A = \frac{hh_{nc}^2}{t_w}, B = -\frac{3Lhh_{nc}}{t_w}, C = \left(\frac{2h(L^2 - h_{nc}^2)}{t_w} + \frac{2(h - h_{nc})^2 L^2}{A_b} + \frac{(4h + 5h_{nc})(h - h_{nc})^5 L}{720I_c h} \right),$$

$$D = \frac{2Lhh_{nc}}{t_w} + \frac{hh_{nc}^3}{A_c}, E = -\frac{3hh_{nc}^2}{t_w} - \frac{3h^2Lh}{A_c}, F = \frac{5Lhh_{nc}}{t_w} + \frac{3L^2hh_{nc}}{A_c}, G = -\frac{2L^2h}{t_w} - \frac{hL^3}{A_c}$$
(26)

Eq. (27) shows that by substituting h_{nc} with zero, Eq. (26) results the Timler and Kulak equation which is used by AISC341-16 ((F5-2) Eq. in AISC 341).

Fig. 19 depicts Eq. (26) results versus finite element model results calculated by averaging the principal stress inclinations angle in path defined in Fig. 16. As it is observed, Eq. (26) accurately predicts α in a post buckled elastic state by about 4-degrees error. This state typically happened in the drift ratio range of 0.2–0.5% (Webster et al. [34]) if no inelastic loading has already occurred.

Relevant studies indicated that the drift yield angle (γ_y) of SPSW is relatively small ($\gamma_y = \frac{2\epsilon_y}{\sin(2\alpha)} \approx 2\epsilon_y = 2 \times \frac{\sigma_y}{E} = 2 \times \frac{328.3}{2 \times 10^5} \approx 0.3\%$) [37].

It is noted that Park R method [6,38] was used to determine the yield displacement based on numerical push-over curve. Force-displacement diagrams of the small-scale specimens and the results from Abaqus analyses of the specimens are shown in Fig. 20. Good agreement between

the experimental and numerical results is observed in this figure. As it is observed, the value predicted by Eqs. (7) and (26) determine the shear yield strength of the steel wall with a good accuracy (Table 5). Actual angle of inclination of the tension field is obtained from the average measurements taken along the crests of the buckled strips. Table 6 shows that the predicted values of inclination angle are in good accordance with the experimental ones. (Eq. (26)). It needs to be noted that it was assumed that the web plate remains in elastic range while measuring the

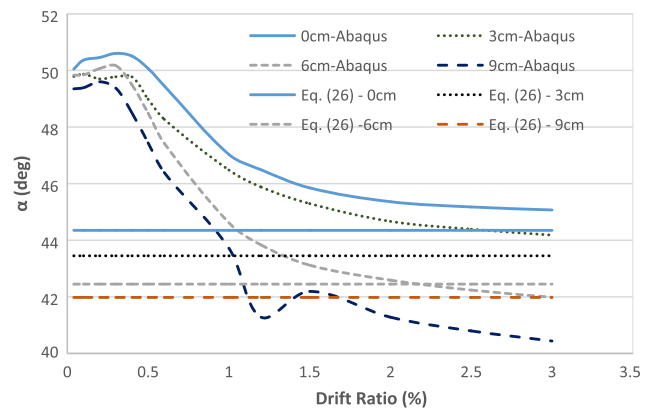


Fig. 19. Migration of inclination angle of the web plate with respect to inter-story drift ratio.

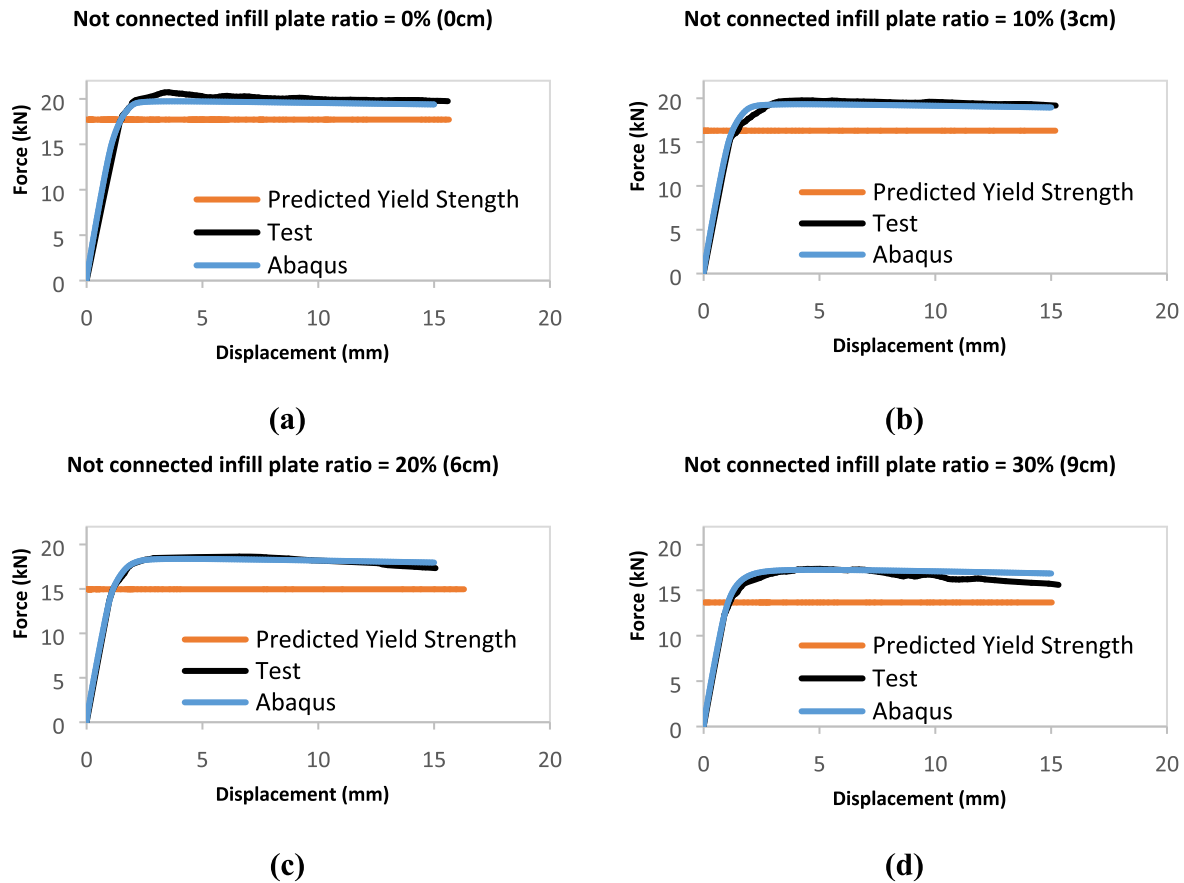


Fig. 20. Force-displacement diagrams of the four small-scale test specimens.

Table 6
Predicted values vs. actual values of shear yield strength.

<i>h</i> (cm)	<i>L_{cf}</i> (cm)	<i>t_w</i> (cm)	<i>h_{nc}</i> (cm)	$\tan \alpha$ (Eq. (26))	α (Eq. (26)-deg)	<i>F_y</i> (MPa)	<i>V_y</i> (kN)	α (actual-deg)	<i>V_y</i> (α (actual))
30	36	0.03	0	0.98	44.35	328.3	17.72	45	17.73
30	36	0.03	3	0.95	43.45	328.3	16.30	43	16.3
30	36	0.03	6	0.91	42.45	328.3	14.96	43	14.93
30	36	0.03	9	0.90	41.98	328.3	13.66	44	13.44

angles of tension field inclination. As it is observed, wall shear strength is conservatively calculated based on Eq. (7) according to comprehensive discussion presented about Fig. 11. Phenomenon. Based on Table 6 data, Fig. 21. illustrates calculated value for effective width of web plate central part (*L_{cf}*-*L_{Neff}*) in Fig. 17. As it can be visually observed *L_{cf}*-*L_{Neff}* value has the same value by the plateau length on Fig. 17. Which demonstrates effective part in section 1–1 which act in stress mobilizing.

6. VBE minimum stiffness requirements as a validating method to prove formation of uniform tension field stress in web plate

To ensure the formation of almost uniform tension field across the infill plate, it is necessary that the vertical boundary elements have minimum specified stiffness (sufficient moment of inertia). In conventional steel shear wall, minimum stiffness requirement of VBE was developed based on Wagner’s analytical studies on aluminum girders with very thin metal webs subjected to transverse shear [39] as SPSW and thin-web plate girders perform similarly in many respects.

For plate girders with infinitely rigid flanges in bending, there would be no local deflections of flanges between neighboring stiffeners due to the formation of tension field in the web plate. As a result, a uniform

tension field is formed across the entire web plate. To model the flexibility of the plate girder flange, it is assumed to be a fixed end beam (Length = spacing between adjacent stiffeners in a plate girder) which is simplified instead of continuous beam located on elastic foundations. Furthermore, a more realistic load distribution along each flange was calculated.

Based on Wagner’s analytical investigation, stress uniformity ratio, $\sigma_{mean} / \sigma_{max}$, was derived as:

$$\frac{\sigma_{mean}}{\sigma_{max}} = \left(\frac{2}{\omega_t}\right) \left[\frac{\cosh(\omega_t) - \cos(\omega_t)}{\sinh(\omega_t) + \sin(\omega_t)}\right] \tag{28}$$

where σ_{mean} = mean of the infill plate tension force components parallel with the HBE, σ_{max} = maximum of the infill plate tension force components parallel with the HBE, ω_t = flexibility factor, defined as: $\omega_t = \sin(\alpha) \sqrt[4]{\frac{I_w}{4L I_{eq}}} h$, *h* = spacing between adjacent stiffeners in a plate girder (which corresponds by analogy with the story height of a SSW), *t_w* = web plate thickness, *L* = depth of the plate girder which corresponds by analogy with the width of a SSW, α = inclination angle of the web plate tension action, $I_{eq} = I_f / 2$ is the equivalent moment of inertia of flange (which corresponds by analogy with equivalent moment of inertia of

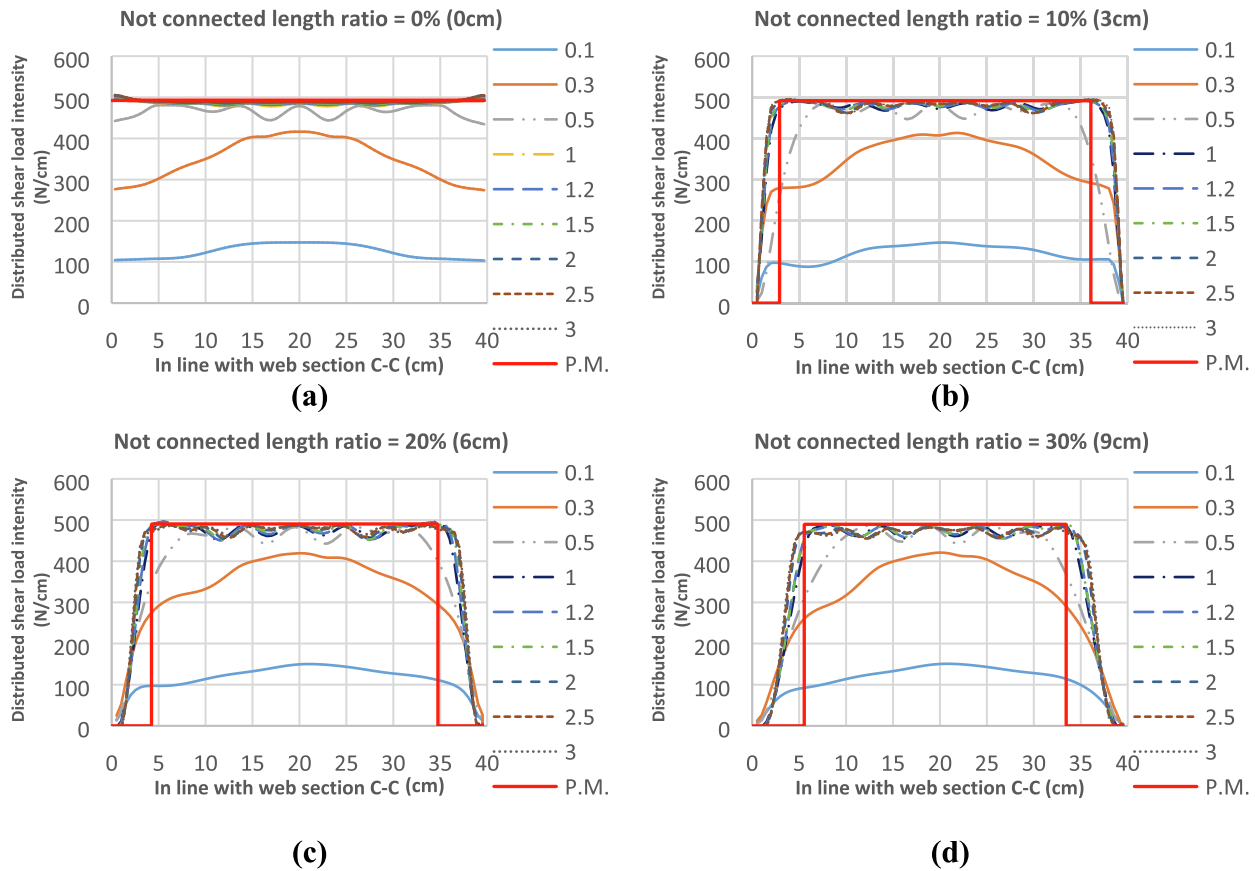


Fig. 21. Distributed shear load intensity due to tension field stress ($\sigma_{12} \times t_w$) along the web plate cross section cut (section C–C in Fig. 10.) with respect to percent of interstory drift ratio, versus proposed method (P.M.) calculated value for effective width of web plate central part ($L_{cf}L_{Neff}$) a) S1; b) S2; c) S3; d) S4.

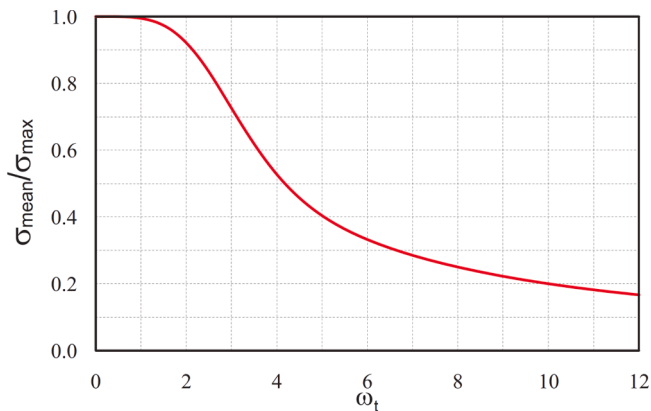


Fig. 22. Relationship between flexibility factor and stress uniformity ratio [41]

column - $I_{eq} = I_C / 2$, E is the modulus of elasticity.

This flexibility factor was introduced to represent the flexibility deformation of the girder flange.

As a result, to ensure the adequacy of VBEs stiffness requirements, CSA S16-01 (CSA, 2001) [40] introduced ω_b , proposed in previous analytical work of plate girder theory and later used in the analogy of steel plate shear wall, as an index of VBE flexibility which in Wagner study shows flanges flexibility.

CSA S16 [40] implicitly limits the decrease of the infill plate average stress (σ_{mean}) to approximately 17% of maximum stress (σ_{max}) by assigning $\omega_t = 2.5$, which is also accepted by AISC 341 [33].

Fig. 22 shows the relationship between the stress uniformity ratio

($\sigma_{mean}/\sigma_{max}$) and the flexibility factor (ω_t). As shown, for smaller values of ω_t (e.g., in the range $0 \leq \omega_t \leq 1$), for which the steel shear wall possesses relatively stiff columns, the stress uniformity ratio is nearly equal to 1, which physically means that the maximum stress is close to the average stress. Therefore, it reveals the development of a uniform infill tension field. However, with an increase in the flexibility factor, the stress uniformity ratio decreases, indicating the formation of a less uniform infill tension field in steel shear walls possessing more flexible columns [41].

This section of the research project aims to determine the minimum required flexural stiffness for shear walls with partial length connection of infill plate to vertical boundary element. However, the relationship between the VBE deformation and the said flexibility parameter is not explicitly described. Therefore, in this study, the flexibility parameter is further converted to the inward deflection at the same location (SL) of the VBE for the fully connected SPSW which is introduced in what follows.

It is noteworthy that by the analogy with boundary condition of the flange between two stiffeners in Wagner’s modeling, fixed end boundary condition for VBE between lower and higher HBE are considered (see Fig. 23.).

Where, η_L and η_R are the flexural deflections of the left and right columns within the story height, respectively and q_r = horizontal components of tension field distributed force parallel with the HBE)

For this purpose, equal stress uniformity ratio ($\sigma_{mean} / \sigma_{max}$) is considered to be at the same location (SL) on fully connected infill plate to vertical boundary element and partially connected infill plate to vertical boundary element steel shear wall, as illustrated in Fig. 24.

Where $y_{SP} = h \frac{(1-NCR)}{2}$ is at the same location point on fully connected steel shear wall;

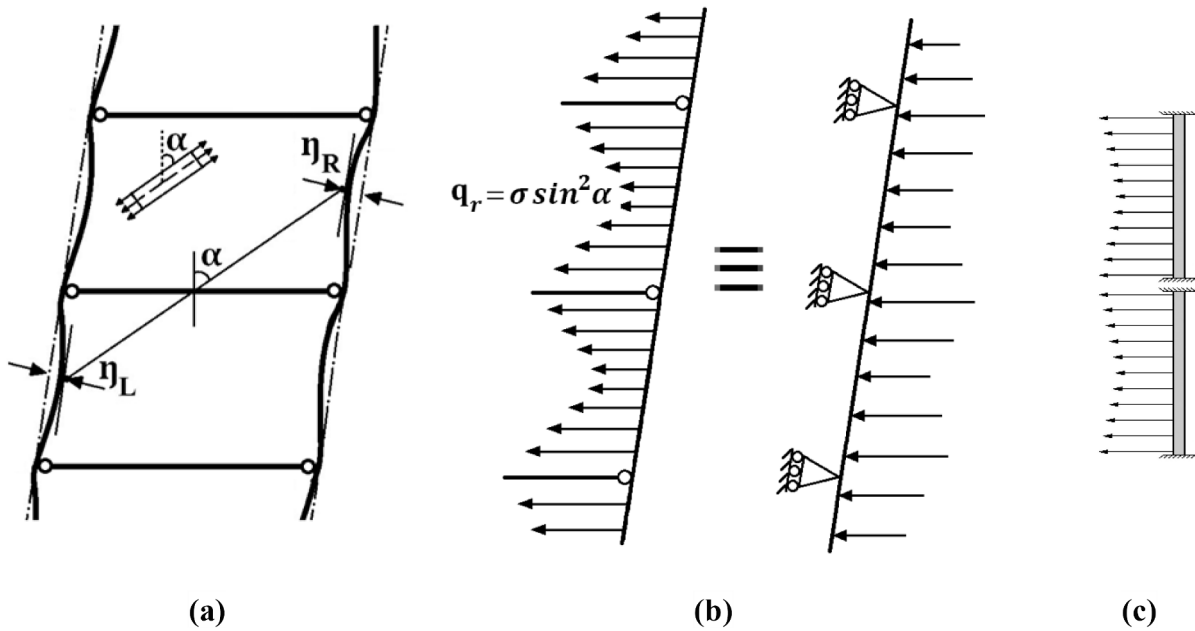


Fig. 23. Fixed end Modeling of VBE based on Wagner assumption for plate girder; (a) SSW, VBE inward flexural deflection, (b) modeling each VBE of the SSW as a continuous beam, (c) simplified fixed end VBE boundary condition.

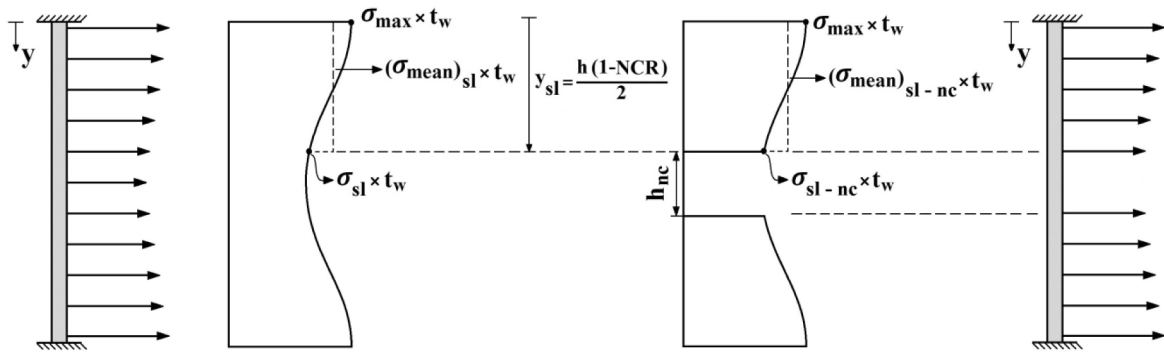


Fig. 24. Same location approach to determine required flexural stiffness of partially connected infill plate to vertical boundary element steel shear wall.

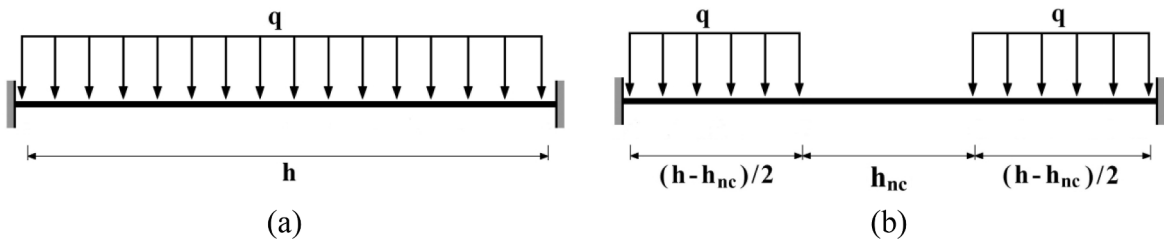


Fig. 25. VBE stiffness requirement simplified modeling; (a) coventinal SPSW, (b) partially connected steel shear wall.

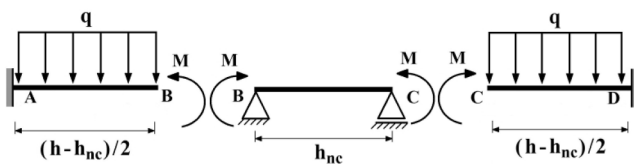


Fig. 26. Components of vertical boundary element and corresponding loadings.

Table 7
VBE minimum stiffness (moment of inertia) requirement $C \cdot 10^{-3} (t_w h^4 / L)$.

NCR	C	Reduction (%)
0	3.1	0
0.05	2.79	10.0
0.1	2.49	19.7
0.15	2.20	28.98
0.2	1.93	37.78
0.25	1.67	46
0.3	1.44	53.6

σ_{SL} = infill plate tension force components parallel to the HBE at the same location on fully connected infill plate to vertical boundary element steel shear wall;

$(\sigma_{mean})_{SL}$ = mean of the infill plate tension force components parallel to the HBE between the same location point and VBE to HBE connection point on fully connected infill plate to vertical boundary element steel shear wall;

σ_{SL-nc} = infill plate tension force components parallel to the HBE at the same location point on partial length connection of infill plate to vertical boundary element steel plate shear walls;

As previously mentioned in CSA S16-01, the stress uniformity ratio has been implicitly taken higher than 83%. Based on Wagner’s assumption, the minimum stress is formed at the middle of plate girder flanges between two stiffeners corresponding by analogy with the middle of VBE height between lower and higher HBE. Regarding this discussion, the same location approach in partially connected SPSW causes the stress uniformity ratio to be higher than 83% as a simple assumption, illustrated in Fig. 25, resulted in uniform distributed load with an intensity of $q = R_y F_y t_w \sin^2(\alpha)$. Due to the correlation of displacement and web plate induced stress at the same location of VBE, equal displacement value in the same location approach was employed instead.

For the analysis of the simplified model shown in Fig. 25b. VBE model (the aim of this research), the displacement compatibility equation method is used (Fig. 26.). Compatibility equation is satisfied when the various segments of the structure fit together without intentional breaks or overlaps.

Eq. (29) presents compatibility equation for rotation at B point (Fig. 26). By substituting load–displacement equation with compatibility equation (Eq. (30)), unknown redundant moment (M_B) can be obtained (Eq. (31))

$$\theta_{LB} = \theta_{RB} \tag{29}$$

$$\frac{q \left(\frac{h - h_{nc}}{2} \right)^3}{6EI_{nc}} - \frac{M_B \left(\frac{h - h_{nc}}{2} \right)}{EI_{nc}} = \frac{M_B h_{nc}}{2EI_{nc}} \tag{30}$$

$$M_B = \frac{q(h - h_{nc})^3}{24h} \tag{31}$$

where I_{nc} = minimum required moment of inertia for VBE in partial length connection SPSW and $I = 0.0031 t_w h^4 / L$ [33] is the minimum required moment of inertia for VBE in conventional SPSW.

As mentioned, by taking equal displacements in two types of SPSW at the same locations,

Fig. 25.a and.b which correspond to Eqs. (32) and (33), respectively, required VBE stiffness of partially connected SPSW is derived based on Eq (34).

$$\delta_{x=\frac{h-h_{nc}}{2}} = \frac{qx^2}{24EI}(h-x)^2 = \frac{q(h-h_{nc})^2}{384EI}(h+h_{nc})^2 \tag{32}$$

$$\delta_{sl-nc} = \frac{q \left(\frac{h - h_{nc}}{2} \right)^4}{8EI_{nc}} - \frac{q(h - h_{nc})^3}{24h} \times \frac{\left(\frac{h - h_{nc}}{2} \right)^2}{2EI_{nc}} = \frac{q(h - h_{nc})^4(h + 2h_{nc})}{384EI_{nc}h} \tag{33}$$

$$\delta_{sl-nc} = \delta_x \Rightarrow \frac{I_{nc}}{I} = \frac{q(h - h_{nc})^4(h + 2h_{nc})}{384Eh} \Rightarrow I_{NC} = I \frac{(1 - NCR)^2(1 + 2NCR)}{(1 + NCR)^2} \tag{34}$$

Table 7 determines minimum flexural stiffness (moment of inertia) requirement of VBE based on the above-mentioned calculations.

7. Conclusions

Analytical studies were conducted based on experimental and numerical evidence so as to investigate the effects of various range of not connected length ratio of infill plate to middle height of vertical boundary element on system governing equations. The main factor investigated in experimental and numerical study was the quality of tension field formation in infill plate. The most important results of this research project are outlined below.

- (1) Formation of parallel tension strips in the infill plate of the steel shear wall with partial length connection to vertical boundary elements was experimentally and numerically confirmed for the entire infill plate in case, not connected length ratio is less than 30%.
- (2) Deviation of tension field inclination angle due to increasing of not connected ratio was discussed by comprehensive numerical study.
- (3) Shear strength of the infill plate (with the limit state of shear yielding) was determined and validated experimentally. The proposed equation was derived using the plastic analysis of the strip model. As discussed, modified infill plate shear strength (V_m) decreases linearly by increasing not connected length ratio ($NCR = h_{nc} / h$).
- (4) Inclination angle of the tension field within the infill plate of an unstiffened shear wall subjected to transverse loading is derived using the least work principle and was experimentally validated.
- (5) Minimum stiffness requirement of VBE is developed based on new approach for proposed steel shear wall, in order to ensure the formation of almost uniform tension field across the infill plate.
- (6) Some suggestions for future researches are outlined below:
 - Effect of panel aspect ratio variation on quality of tension strips formation in web plate.
 - Effect of number of stories variation on quality of tension strips formation in web plate.
 - Effect of not connected length ratio on cyclic ductility of proposed steel shear wall.
 - Effect of not connected part connection detailing on ductility and avoiding premature tearing.

Declaration of Competing Interest

The authors declare that they have no known competing financial interests or personal relationships that could have appeared to influence the work reported in this paper.

References

- [1] Astanah-Asl A. Seismic behavior and design of steel plate shear walls, Steel TIPS Report. Structural Steel Educational Council, Moraga, California, 2001.
- [2] Shekastehband B, Azaraxsh A-A, Showkati H, Pavir A. Behavior of semi-supported steel shear walls: experimental and numerical simulations. *Eng Struct* 2017;135: 161–76.
- [3] Hajimirsadeghi M, Mirtaheri M, Zandi A-P, Hariri-Ardebilil M-A. Experimental cyclic test and failure modes of a full scale enhanced modular steel plate shear wall. *Eng Fail Anal* 2019;95:283–8.
- [4] Paslar N, Farzampour A, Hatami F. Investigation of the infill plate boundary condition effects on the overall performance of the steel plate shear walls with circular openings. *J Struct* 2020;27:824–36.
- [5] Yu J-G, Yu H-S, Feng X-T, Dang C, Hou T-F, Shen J. Behaviour of steel plate shear walls with different types of partially-encased H-section columns. *J Constr Steel Res* 2020;170:10612.
- [6] Cui J-C, Xu J-D, Xu Z-R, Huo T. Cyclic behavior study of high load-bearing capacity steel plate shear wall. *J Constr Steel Res* 2020;172:106178.
- [7] Berman J-W, Bruneau M. Experimental Investigation of Light-Gauge Steel Plate Shear Walls for the Seismic Retrofit of Buildings. Technical Report MCEER-03-001, Multidisciplinary Center for Earthquake Engineering Research, Buffalo, NY, (2003a).
- [8] Berman J-W, Lowes L-N, Okazaki T, Bruneau M, Tsai K-C, Driver R-G, Sabelli R, and Moore W-P. Research needs and future directions for steel plate shear walls. In Proceeding of the 2008 Structures Congress.

- [9] Vian D, Bruneau M. Steel Plate Walls for Seismic Design and Retrofit of Building Structures. Technical Report MCEER-05-0010, Multidisciplinary Center for Earthquake Engineering Research, State University of New York at Buffalo, Buffalo, NY, 2005.
- [10] Baftchi H. Analytical and experimental study of aluminum shear panels for retrofitting of existing structures. M.Sc. Thesis, K.N. Toosi University of Technology, Tehran, Iran, 2014.
- [11] Hitaka T, Matsui C. Experimental study on steel shear wall with slits. *J Struct Eng* 2003;129(5):586–95.
- [12] Li C-H, Tsai K-C, Lin C-H, Chen P-C. Cyclic tests of four two story narrow steel plate shear walls. Part 2: experimental results and design implications. *J Earthquake Eng Struct Dyn* 2010;39(7):801–26.
- [13] Dastfan M. Ductile steel plate shear walls with PEC columns. Ph.D. Thesis, University of Alberta, Edmonton, (2011).
- [14] Zhao Q, and Astanah-Asl A. Cyclic behavior of an innovative steel shear wall system. 13th World Conference on Earthquake Engineering, Vancouver, B.C., Canada, August 1-6, 2004, Paper No. 2576. (2004).
- [15] Choi I-R, Park H-G. Cyclic loading test for reinforced concrete frame with thin steel infill plate. *J Struct Eng* 2010;137(6):654–64.
- [16] Jahanpour A, Jonson J, Moharrami H. Seismic behavior of semi-supported steel shear walls. *J Constr Steel Res* 2012;74:118–33.
- [17] Astanah-Asl A. Seismic behavior and design of composite steel plate shear walls, Steel TIPS Report. Structural Steel Educational Council, Moraga, California, 2002.
- [18] Wei M-W, Liew J-Y-R, Du Y, Fu X-Y. Shear resistance of buckling of restrained steel plate shear walls. *Int J Steel Struct* 2017;17(3):1233–48.
- [19] Rahnavard R, Hassanipour A, Mounesi A. Numerical study on important parameters of composite steel-concrete shear walls. *J Constr Steel Res* 2016;121:441–56.
- [20] Guo L, Rong Q, Ma X, Zhang S. Behavior of steel plate shear wall connected to frame beams only. *Int J Steel Struct* 2011;11(4):467–79.
- [21] Choi I-R, Park H-G. Steel plate shear walls with various infill plate designs. *J Struct Eng* 2009;135(7):785–96.
- [22] Qian X, Astanah-Asl A. Development of a high-performance steel plate shear wall system. *Int J Earthquake Impact Eng* 2016;1(1-2):57–80.
- [23] Wei M-W, Liew J-Y-R, Xiong M-X, Fu X-Y. Hysteresis model of a novel partially connected buckling-restrained steel plate shear wall. *J Constr Steel Res* 2016;125:74–87.
- [24] Wei M-W, Liew J-Y-R, Fu X-Y. Panel action of novel partially connected buckling-restrained steel plate shear walls. *J Constr Steel Res* 2017;128:483–97.
- [25] Wei M-W, Liew J-Y-R, Du Y, Fu X-Y. Experimental and numerical investigation of novel partially connected steel plate shear walls. *J Constr Steel Res* 2017;132:1–15.
- [26] Wei M-W, Liew J-Y-R, Du Y, Fu X-Y. Seismic behavior of novel partially connected buckling-restrained steel plate shear walls. *Soil Dyn Earthquake Eng* 2017;103:64–75.
- [27] Pashar N, Farzampour A, Hatami F. Infill plate interconnection effects on the structural behavior of steel plate shear walls. *Thin-Walled Struct* 2020;149:106621.
- [28] Berman J-W, Bruneau M. Capacity design of vertical boundary elements in steel plate shear walls. *Eng J-Am Inst Steel Constr* 2008;45:57–71.
- [29] Shames I-H. *Mechanics of fluids*. 4th Edition. McGraw-Hill; 2002.
- [30] Hibbitt, Karlsson and Sorensen. *Abaqus standard user's manual*, Inc. vols. 1, and 3. Version 6.8-1, 2008.
- [31] Driver R-G, Kulak G-L, Kennedy D-J-L, Elwi A-E. Seismic behavior of steel plate shear walls. Structural Engineering Rep. No. 215, Dept. of Civil and Environmental Engineering, Univ. of Alberta, 1997.
- [32] Berman J-W, Bruneau M. Plastic analysis and design of steel plate shear walls. *J Struct Eng* 2003;129(11):1448–56.
- [33] AISC. Seismic provisions for structural steel buildings. ANSI/AISC 341–16, American Institute of Steel Construction, Chicago, IL, 2016.
- [34] Webster D-J, Berman J-W, Lowes L-N. Experimental investigation of SPSW web plate stress field development and vertical boundary element demand. *J Struct Eng* 2014;140(6):04014011.
- [35] Thorburn L-J. Analysis and Design of Steel Shear Wall Systems. Ph.D. Dissertation. Department of Civil Engineering, University of Alberta, Edmonton, 1982.
- [36] Timler P-A. Experimental study of steel plate shear walls. Ph.D. Dissertation, Department of Civil Engineering, University of Alberta, Edmonton, 1984.
- [37] Bruneau M, Uang C-M, Sabelli S-R. *Ductile design of steel structures*. McGraw-Hill; 2011.
- [38] Park R, Paulay T. *Reinforced Concrete Structures*. John Wiley and Sons Inc, New York, 1975.
- [39] Wagner H. Flat sheet metal girders with very thin metal web. Part III: sheet metal girders with spars resistant to bending-the stress in uprights-diagonal tension fields, NASA Technical Reports Server, Technical Memorandum NO.604, National Advisory Committee for Aeronautics, Washington, DC, 1931.
- [40] CSA, Design of steel structures, CAN/CSA-S16-01, Canadian Standards Association Toronto, Canada, 2001.
- [41] Qu B, Bruneau M. Behavior of vertical boundary elements in steel plate shear walls. *Eng J-Am Inst Steel Constr* 2010;47(2):109–22.